Table 2. Distribution of human hematopoietic cells in IBM or intravenously injected NOD/SCID mice

	Percentage of human CD45+ cells				Lymphoid		Myeloid		Stem/progenitor	
Mouse	Right	Left	Spl	PB	Right	Left	Right	Left	Right	Left
IBM										
1	44.21	0.60	2.46	ND	67.13	63.26	6.96	18.68	28.94	13.98
2	15.83	12.00	0.85	ND	82.82	82.79	3.64	9.54	19.62	6.09
3	34.85	77.90	34.65	ND	69.43	59.60	4.39	5.57	20.66	29.92
4	55.73	50.43	31.92	ND	62.21	68.69	7.22	8.96	19.86	22.83
5	17.57	4.76	2.42	ND	69.35	70.87	8.62	16.00	26.59	22.68
6	77.81	84.74	41.83	14.48	65.16	84.50	31.78	8.53	13.29	22.75
7	96.07	34.23	34.15	11.67	67.21	63.01	14.64	13.89	24.83	21.56
8	28.40	1.84	4.33	0.97	57.12	62.66	12.41	10.76	12.84	10.89
9	39.11	1.87	4.04	2.05	70.45	68.73	4.71	5.96	22.37	28.04
Mean (± SD)	45.51 (26.96)	29.82 (33.79)	17.41 (17.52)	7.29 (6.79)	67.88 (6.99)	69.35 (8.88)	10.49 (8.79)	10.88 (4.47)	21.00 (5.48)	19.86 (7.91)
Intravenous										
1	49.10	52.46	39.18	8.19	74.02	75.04	14.40	11.50	12.71	19.36
2	32.29	21.77	3.64	1.97	86.51	85.86	4.08	5.07	6.00	9.03
3	42.37	39.48	18.35	5.52	69.54	71.22	6.99	9.32	11.59	14.02
4	22.69	16.63	9.20	2.01	86.32	73.07	10.38	12.67	19.31	21.79
5	28.16	22.76	21.16	4.85	80.36	79.76	13.65	15.07	16.88	14.22
6	19.67	22.54	7.55	1.36	68.41	65.59	7.98	11.65	19.28	16.71
7	12.90	8.92	6.50	1.74	62.05	95.64	30.65	3.18	11.18	9.29
Mean (± SD)	29.6 (12.77)	26.37 (14.72)	15.08 (12.41)	3.66 (2.58)	75.32 (9.40)	78.03 (10.08)	12.59 (8.76)	9.78 (4.26)	13.85 (4.89)	14.92 (4.79)

BM cells, spleen cells, and PB of NOD/SCID mice 6 to 9 weeks after iBM or intravenous transplantation of column-enriched but unsorted whole CD34+ cell populations (20 000 cell for iBM and 200 000 cells for intravenous) were stained with antihuman CD45 mAbs and analyzed. BM cells were collected separately from injected (right leg) and noninjected (left leg) side tibia. Lymphoid, myeloid, and stem/progenitor cell lineages are defined as CD19+/CD45+ cells, CD33+/CD45+ cells, and CD34+/CD45+ cells, respectively, and each number indicates the percentage of human CD45+ cells expressing respective surface marker. The proportion of each lineage was calculated from 50 000 to 100 000 events acquired using CELLQuest software.

ND indicates not determined.

of sum of 2 legs], $P = .14$). Human hematopoietic cells were also detected in noninjected side tibia, spleen, and PB of $Lin^{-/low}CD34^+CD38^-$ cells transferred to NOD/SCID mice (Table 3). As few as 5 $Lin^{-/low}CD34^+CD38^-$ cells successfully engrafted in the noninjected side tibia (data not shown). These results suggested that the engrafted human hematopoietic cells in the injected side BM migrate to a noninjected BM by blood flow circulation and differentiate into multilineage cells even when the human hematopoietic cell chimerism showed low level.

Clonal analysis of engrafted human hematopoietic cells transplanted by iBM injection

Relatively high frequencies of human hematopoietic cells found in noninjected BM might suggest that cells entering the blood stream because of the pressure applied in iBM procedure or release after engraftment in injected side tibia. Although we found little evidence of leakage (Figure 2), we proceeded in examining the clonalities of cells present in different hematopoietic organs. Retroviral gene marking provides the ideal tool for studies of clonal analysis because they randomly and permanently integrate into the genome of the host cell. Thus, each genomic integration site is a distinct clonal marker that can be used to trace the progeny of individual stem cells after transplantation.[19,23-25] Therefore, we transduced the *EGFP* gene to CB $CD34^+$ cells by lentiviral infection and transplanted them into NOD/SCID mice by iBM injection. Eight weeks after transplantation, BM and spleen were isolated and analyzed by flow cytometry. BM cells were isolated separately from tibiae of injected side and noninjected side. High frequencies of $EGFP^+$ cells were demonstrated in the engrafted mice (61.16% ± 23.99%, n = 4) (Figure 5A). As shown in Figure 5B, common clones were evident among the injected side BM and other hematopoietic organs. The results suggest that HSCs, directly injected into BM, engraft in the marrow environment and migrate to other hematopoietic organs by mobilization through a systemic circulation.

Table 3. Distribution of human hematopoietic cells ($CD34^+CD38^-$) in iBM-injected NOD/SCID mice

	Percentage of human CD45+ cells			
No. cells	Injected tibia	Noninjected tibia	Spleen	PB
10 000	86.13	57.91	64.68	27.86
1 000	33.62	5.28	3.80	0.85
500	47.94	1.28	2.44	ND
250	5.00	0.10	0.10	0.04
100	5.58	0.12	0.35	0.02

BM cells, spleen cells, and PB of NOD/SCID mice 8 weeks after transplantation of CB $Lin^{-/low}CD34^+CD38^-$ cells by iBM were stained with antihuman CD45 mAbs and analyzed. BM cells were collected separately from tibiae of injected and noninjected side.

ND indicates not determined.

Higher engraftment in secondary NOD/SCID mice that received transplants by iBM injection

Self-renewal of hematopoietic stem cells can be assessed by serial transplantation in SRC assay. A theory behind this assay is that stem cells which give rise to multilineage hematopoiesis in primary recipients are also capable of repeating this process in recipients of secondary transplants. The proportion of human cells in the secondary mice, however, is usually more than 10 times lower than in the primary mice. Consistent with previous studies, secondary mice that received intravenous transplants showed low levels of engraftment (Figure 6A). In contrast, engraftment levels in secondary recipients were significantly higher when they received transplants by iBM (Figure 6B; the reduction rate in chimerism from first to second recipients is 0.031 ± 0.018 in intravenous versus 0.546 ± 0.268 in iBM; $P < .01$). Thus, human cells recovered

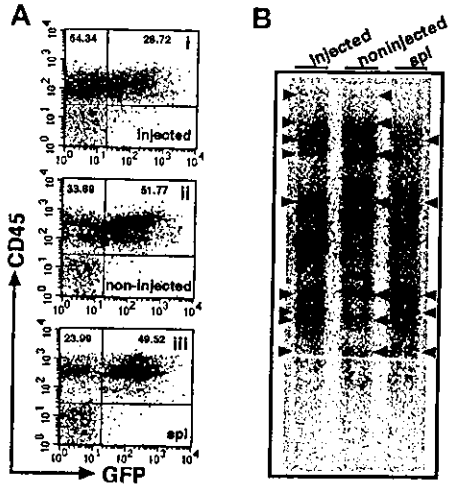

Figure 5. Clonal analysis of iBM-injected SRCs. (A) The proportion of EGFP+ human cells was analyzed at 8 weeks after iBM transplantation. Samples were obtained from injected side tibia (i), noninjected side tibia (ii), and spleen (iii). Cells were stained with antihuman CD45 mAb and analyzed by flow cytometry. Representative FACS profiles are shown from 4 independent experiments. The relative frequencies of each population are indicated. (B) Southern blot analysis for lentivirus integration sites. Genomic DNA extracted from samples indicated earlier was digested with *Eco*RI, which recognizes a unique site in lentivirus vector, and was hybridized with an EGFP probe. Each band represents a unique lentiviral integration site, and it corresponds to each clone. Arrowheads indicate common integration sites. Representative Southern blot analysis of 2 independent experiments is shown.

from BM of primary NOD/SCID mice that received iBM transplants possessed sufficient ability for consecutive multilineage engraftment in secondary recipients (Figure 6C), suggesting that human HSCs transplanted by iBM injection can self-renew in murine BM.

Engraftment of CD34+ cells by iBM injection is dependent on CXCR4, VLA-4, and VLA-5

Stem cell engraftment involves multistep processes, including activation of specific adhesion molecules. A number of studies have

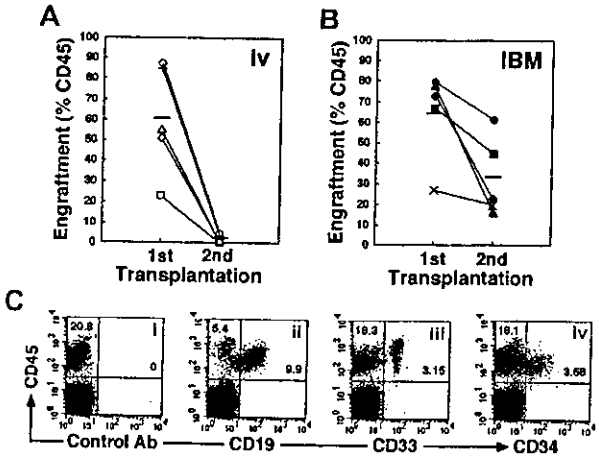

Figure 6. Secondary transplantation. (A-B) Whole human BM cells obtained from each primary recipient mouse given an iBM transplant (n = 10) were transplanted to a secondary recipient mouse by intravenous injection (n = 5) (A) or iBM injection (n = 5) (B). Secondary recipient mouse BM cells were analyzed for the expressions of human CD45 at 6 weeks after transplantation. Each symbol represents 1 mouse, and bars indicate the average engraftment level in 3 independent experiments. (C) Representative FACS analysis of a NOD/SCID mouse that received a secondary transplant. Human CD45+ cells in BM were analyzed for the expression of CD19 (ii), CD33 (iii), and CD34 (iv). The relative frequencies of each population are indicated.

reported crucial roles of VLA-4, VLA-5, and other molecules in interaction of HSCs and microenvironment during homing and engraftment processes (reviewed in Prosper and Verfaillie[26] and in Lapidot[27]). Up-regulation of these molecules through SDF-1–CXCR4 (stromal cell–derived factor 1 and CXC chemokine receptor 4) interaction is reported to increase homing and engraftment of primitive SRCs.[27-29] Primitive human CB CD34+ cells express a chemokine receptor CXCR4 and major β1 integrin VLA-4 and VLA-5 (Figure 7A). The iBM transplantation offers the opportunity to investigate the interaction between stem cells and BM stromal cells in vivo by eliminating the processes before entering marrow environment. To determine the in vivo role of CXCR4, VLA-4, and VLA-5 during the engraftment process of human SRCs, enriched CB CD34+ cells were pretreated with antibodies against the cell surface molecules mentioned and then transplanted. When CB CD34+ cells were transplanted intravenously, neutralizing antibodies to CXCR4, VLA-4, and VLA-5 completely blocked BM engraftment as described previously (Figure 7, indicated as open circles, $P < .01$),[27-29] whereas neutralizing antibodies to either VLA-4 or VLA-5 caused only partial inhibition of engraftment in iBM transplants (Figure 7, indicated as filled circles, $P < .05$). However, when CD34+ cells were pretreated with anti-CXCR4 or with both anti–VLA-4 and anti–VLA-5 antibodies, human SRCs engraftment was blocked completely (Figure 7, indicated as filled circles, $P < .01$).

Discussion

Primitive human hematopoietic cells can be assayed on the basis of their ability to repopulate immune-deficient NOD/SCID mice and have been termed SCID-repopulating cells (SRCs).[1-3] By using this

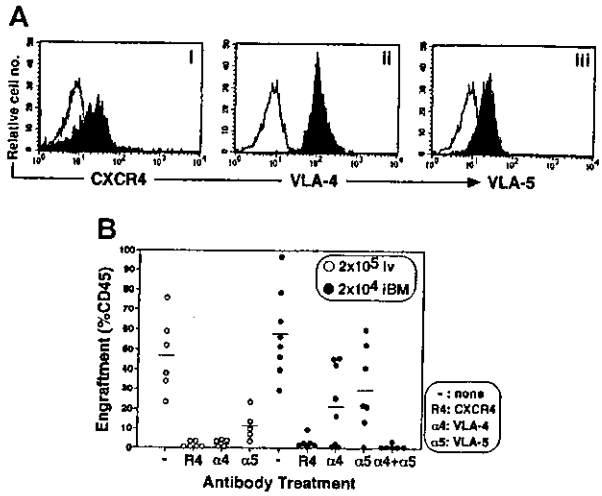

Figure 7. Effect of antibodies to CXCR4 and β1 integrins on engraftment of cord blood CD34+ cells in NOD/SCID mice BM. (A) Expression of CXCR4 (i), VLA-4 (ii), and VLA-5 (iii) on enriched CD34+ cells. Expression levels of CXCR4, VLA-4, and VLA-5 on gated CD34+ population are shown. A representative FACS analysis of 3 independent experiments is shown. The white histogram indicates negative control staining with isotype control antibody; the black histogram indicates CXCR4 (i), VLA-4 (ii), and VLA-5 (iii). (B) Percentage of engraftment in murine BM by CB CD34+ cells pretreated with antibodies to either CXCR4 (R4), VLA-4 (α4), VLA-5 (α5), or VLA-4 + VLA-5 (α4 + α5) was quantified at 6 weeks after transplantation by immunostaining with antihuman CD45 mAb. Open circles (○) represent the mouse that received a transplant of 2×10^5 of CD34+ cells intravenously. Filled circles (●) represent the mouse that received a transplant of 2×10^4 CD34+ cells by iBM. Each circle represents 1 mouse, and bars indicate the average of engraftment. Results were combined from 3 independent experiments.

human-to-mouse xenogeneic transplantation model, studies reported substantially low recoveries of SRCs.[12,13] These results imply that homing of primitive hematopoietic cells to the BM is nonselective and/or an inefficient process. A number of factors, such as entrapment in liver and/or lung, molecular incompatibility between human integrins and its ligands expressed on mouse, would interfere with homing and engraftment of HSCs. Therefore, it has been speculated that if one could eliminate such factors, SRC frequency should become markedly higher than that reported previously.[4,22,30] Here we report that by introducing cells directly into the marrow environment with the use of the iBM method, the frequency of SRCs became more than 15-fold higher (1 in 44 $Lin^{-/low}CD34^+CD38^-$ cells; 95% confidence intervals, 1 in 27 to 1 in 70) than intravenous injection (1 in 660 $Lin^{-/low}CD34^+CD38^-$ cells; 95% confidence intervals, 1 in 289 to 1 in 1510) (Figure 3; Table 1). This finding is compatible with the previous speculation that the SRC frequency could become 10 to 20 times higher, assuming there is no interference. Furthermore, multilineage reconstitution (Figure 4; Table 2) and self-renewal (Figure 6) were demonstrated by human SRCs injected by iBM method. One might argue that iBM injection created a hematoma in the injected site and reflected survival of human cells. However, the results clearly demonstrated maintenance of hematopoiesis as was seen in intravenous injection of human HSCs. Detection of no human cells in mice given transplants of 10^4 irradiated $CD34^+CD38^+$ carrier cells alone also eliminated the former possibility (Figure 3). Furthermore, a mouse given a transplant of 5 human $CD34^+CD38^-$cells showed 0.04% of chimerism in the injected tibia (Figure 3). On the basis of the number of cells recovered from the tibia (2×10^6), a calculated value of human cells was approximately 800, which could represent a 160-fold proliferation of injected cells.

In addition, human hematopoietic cells with the ability of multilineage differentiation were detected in the noninjected side tibia, spleen, and PB (Figure 4; Tables 2-3). In our iBM strategy, there was little, if any, leakage of the injected cells into the peripheral circulation (Figure 2). In much the same way, recently Zhong et al,[31] using the mouse-to-mouse intrafemur injection method, demonstrated that the donor murine cell in PB was undetectable at early points. At the late time points, transplanted donor cells in the noninjected femur were detected as the same level to the injected femur. In our experiments, however, engraftment in the noninjected BM tends to be low (Tables 2-3). The discrepancy may come from the lowering ability of human HSCs to home to the noninjected BM in xenoenvironment. Importantly, we confirmed the existence of common clones in the injected BM and other hematopoietic organs using a retroviral gene marking (Figure 5). We speculate that the human cells introduced directly into the murine marrow environment proliferate, migrate through a physiologic circulatory system, and engraft in other hematopoietic spaces. The level of chimerism may depend on the ability of proliferation and survival in each engrafted clone.[19] Independent clones were also present in the injected side and the noninjected side of legs (Figure 5). There may be 2 possibilities: leakage of HSCs during iBM injection and behavioral differences in SRC clones engrafted in the injected BM. The results of our tracing experiments (Figure 2) strongly support the later possibility. Also, Wright et al[6] demonstrated a dynamic circulation of HSCs. HSCs rapidly and constitutively migrate from BM to blood stream, and this circulation plays a physiologic role in the functional reengraftment of another place of BM. Using this iBM method, we might shed light on the mechanisms of human HSCs homing (noninjected side BM) and engraftment (injected side BM).

Self-renewal is a key characteristic of primitive stem cells and distinguishes them from short-lived progenitor cells. However, assessment of self-renewal in SRC assay requires transplantation into secondary recipients and has been difficult because of the lack of a sensitive and reliable method. Treatment of marrow cells derived from primary recipient mice with interleukin 6 (IL-6) and SCF up-regulated the surface expression of CXCR4 and resulted in higher engraftment levels than those of untreated cells when cells were transplanted in secondary recipients.[28,29] Thus, the expression of CXCR4 appears essential for homing, and therefore engraftment, of human cells. In other words, reduced expression of CXCR4 and other homing-related molecules in primary-engrafted SRCs may be a reason for the diminished level of human cells in a secondary recipient. The iBM strategy we used in this study can disregard the effect of homing factors, and we successfully demonstrated high levels of engraftment and multilineage differentiation of HSCs in secondary recipient (Figure 6).

Homing and lodgement of transplanted HSCs to recipient BM are critical steps in engraftment and initiation of marrow reconstitution. In the first phase "homing," transplanted cells must home to vascular sites and need to penetrate the basal lamina that is composed of extracellular matrix (ECM) proteins. In the second phase "lodgement," HSCs must stay in the appropriate niches of microenvironment where these cells survive, proliferate, and differentiate to reconstitute hematopoiesis, that is, "engraftment." Human HSC engraftment in NOD/SCID mice depends on the expression of the chemokine SDF-1 and its receptor CXCR4.[28,29,32] The SDF-1 activates the integrins lymphocyte function antigen 1 (LFA-1), VLA-4, and VLA-5 on human $CD34^+$ cells. HSCs polarize and migrate through the ECM toward local gradients of SDF-1, which are produced by specialized stromal cells, and orient themselves through the different elements of the BM microenvironment and settle in the stem cell niches.[27,29] Although previous studies showed the inhibition of engraftment in Ab blocking experiments,[28,29,33,34] whether each molecule contributes to either the homing or lodgement step or both has not been clarified, because this system could not differentiate the homing and lodgement. Our iBM strategy is useful to evaluate lodgement as it bypasses the homing step.

In line with the previous studies by Peled et al,[28,29] intravenous injection of human $CD34^+$ cells pretreated with anti-CXCR4, -VLA-4, and -VLA-5 mAbs resulted in complete inhibition of engraftment in NOD/SCID mice (Figure 7). However, the same researchers demonstrated that pretreatment with anti-integrin mAbs reduced homing, but not engraftment, of human cells into BM by approximately 30% to 50%.[32] From these results, we hypothesize that VLA-4 and VLA-5, expressed on HSCs, are involved in part in both homing and lodgement processes. With the use of the iBM strategy, blocking of either VLA-4 or VLA-5 affected engraftment only partially, whereas neutralization of CXCR4 or VLA-4 and VLA-5 together completely inhibited human HSC engraftment (Figure 7). Therefore, engraftment requires interaction between integrins expressed on BM microenvironment and each VLA-4 and VLA-5 expressed on human HSCs. A number of in vitro studies suggested the importance of integrin-mediated signaling pathways for localization of HSC in BM microenvironment[35-39] as well as survival and proliferation of human HSCs.[40-43] To our knowledge, the results of our iBM strategy are the first to demonstrate directly the important in vivo roles of integrins and chemokine receptor for not only homing but also lodgement of HSCs in BM microenvironments. Further studies will determine the molecular mechanisms concerning the HSCs lodgement by our iBM strategy. We are in the

process of examining the molecules participating only in HSC lodgement.

Our study indicates that iBM transplantation is a method that can accurately evaluate the innate ability of human HSCs. By using this highly sensitive method, more primitive human hematopoietic stem cells, including cells that have lower capability for homing, such as Lin^-CD34^- cells,[44,45] can be identified at a single cell level as previously demonstrated in the murine experiment.[46] The iBM method is also suitable to analyze BM cells and mobilized PB cells that exhibit low engraftment capability compared with CB in the SRC assay.[12,22] As shown by Kushida et al,[14,47] the iBM strategy makes it possible to coadministrate hematopoietic and hematopoietic-supporting mesenchymal stromal cells into recipient BM, which in turn may facilitate the human hematopoietic cell engraftment in murine BM. These studies would further our understandings of the mechanisms of homing and engraftment of human HSCs and lead to possible applications in clinical transplantation medicine.

Acknowledgments

We thank Dr Hiroshi Kawada for useful discussion, Hideyuki Matsuzawa and Tomomi Takanashi for technical assistance, Tomoko Uno for secretarial works, members of the animal facility of Tokai University, especially Mitsugu Hirano and Mayumi Nakagawa, for meticulous care of experimental animals, and members of Tokai Cord Blood Bank for their assistance.

References

1. Larochelle A, Vormoor J, Hanenberg H, et al. Identification of primitive human hematopoietic cells capable of repopulating NOD/SCID mouse bone marrow: implications for gene therapy. Nat Med. 1996;2:1329-1337.
2. Cashman JD, Lapidot T, Wang JC, et al. Kinetic evidence of the regeneration of multilineage hematopoiesis from primitive cells in normal human bone marrow transplanted into immunodeficient mice. Blood. 1997;89:4307-4316.
3. Hogan CJ, Shpall EJ, McNulty O, et al. Engraftment and development of human CD34(+)-enriched cells from umbilical cord blood in NOD/LtSz-scid/scid mice. Blood. 1997;90:85-96.
4. Bhatia M, Wang JC, Kapp U, Bonnet D, Dick JE. Purification of primitive human hematopoietic cells capable of repopulating immune-deficient mice. Proc Natl Acad Sci U S A. 1997;94:5320-5325.
5. Cui J, Wahl RL, Shen T, et al. Bone marrow cell trafficking following intravenous administration. Br J Haematol. 1999;107:895-902.
6. Wright DE, Wagers AJ, Gulati AP, Johnson FL, Weissman IL. Physiological migration of hematopoietic stem and progenitor cells. Science. 2001;294:1933-1936.
7. Wagers AJ, Allsopp RC, Weissman IL. Changes in integrin expression are associated with altered homing properties of Lin(-/lo)Thy1.1(lo)Sca-1(+)c-kit(+) hematopoietic stem cells following mobilization by cyclophosphamide/granulocyte colony-stimulating factor. Exp Hematol. 2002; 30:176-185.
8. Jetmore A, Plett PA, Tong X, et al. Homing efficiency, cell cycle kinetics, and survival of quiescent and cycling human CD34(+) cells transplanted into conditioned NOD/SCID recipients. Blood. 2002;99:1585-1593.
9. Wolf NS, Kone A, Priestley GV, Bartelmez SH. In vivo and in vitro characterization of long-term repopulating primitive hematopoietic cells isolated by sequential Hoechst 33342-rhodamine 123 FACS selection. Exp Hematol. 1993;21:614-622.
10. Spangrude GJ, Brooks DM, Tumas DB. Long-term repopulation of irradiated mice with limiting numbers of purified hematopoietic stem cells: in vivo expansion of stem cell phenotype but not function. Blood. 1995;85:1006-1016.
11. van der Loo JC, Ploemacher RE. Marrow- and spleen-seeding efficiencies of all murine hematopoietic stem cell subsets are decreased by preincubation with hematopoietic growth factors. Blood. 1995;85:2598-2606.
12. van Hennik PB, de Koning AE, Ploemacher RE. Seeding efficiency of primitive human hematopoietic cells in nonobese diabetic/severe combined immune deficiency mice: implications for stem cell frequency assessment. Blood. 1999;94: 3055-3061.
13. Cashman JD, Eaves CJ. High marrow seeding efficiency of human lymphomyeloid repopulating cells in irradiated NOD/SCID mice. Blood. 2000; 96:3979-3981.
14. Kushida T, Inaba M, Hisha H, et al. Intra-bone marrow injection of allogeneic bone marrow cells: a powerful new strategy for treatment of intractable autoimmune diseases in MRL/lpr mice. Blood. 2001;97:3292-3299.
15. Verstegen MM, van Hennik PB, Terpstra W, et al. Transplantation of human umbilical cord blood cells in macrophage-depleted SCID mice: evidence for accessory cell involvement in expansion of immature CD34+CD38- cells. Blood. 1998;91:1966-1976.
16. Bonnet D, Bhatia M, Wang JC, Kapp U, Dick JE. Cytokine treatment or accessory cells are required to initiate engraftment of purified primitive human hematopoietic cells transplanted at limiting doses into NOD/SCID mice. Bone Marrow Transplant. 1999;23:203-209.
17. Kawada H, Ando K, Tsuji T, et al. Rapid ex vivo expansion of human umbilical cord hematopoietic progenitors using a novel culture system. Exp Hematol. 1999;27:904-915.
18. Verlinden SF, van Es HH, van Bekkum DW. Serial bone marrow sampling for long-term follow up of human hematopoiesis in NOD/SCID mice. Exp Hematol. 1998;26:627-630.
19. Guenechea G, Gan OI, Dorrell C, Dick JE. Distinct classes of human stem cells that differ in proliferative and self-renewal potential. Nat Immunol. 2001;2:75-82.
20. Oki M, Ando K, Hagihara M, et al. Efficient lentiviral transduction of human cord blood CD34(+) cells followed by their expansion and differentiation into dendritic cells. Exp Hematol. 2001;29: 1210-1217.
21. Cashman JD, Eaves CJ. Human growth factor-enhanced regeneration of transplantable human hematopoietic stem cells in nonobese diabetic/severe combined immunodeficient mice. Blood. 1999;93:481-487.
22. Wang JC, Doedens M, Dick JE. Primitive human hematopoietic cells are enriched in cord blood compared with adult bone marrow or mobilized peripheral blood as measured by the quantitative in vivo SCID-repopulating cell assay. Blood. 1997;89:3919-3924.
23. Dick JE, Magli MC, Huszar D, Phillips RA, Bernstein A. Introduction of a selectable gene into primitive stem cells capable of long-term reconstitution of the hemopoietic system of W/Wv mice. Cell. 1985;42:71-79.
24. Keller G, Paige C, Gilboa E, Wagner EF. Expression of a foreign gene in myeloid and lymphoid cells derived from multipotent haematopoietic precursors. Nature. 1985;318:149-154.
25. Lemischka IR, Raulet DH, Mulligan RC. Developmental potential and dynamic behavior of hematopoietic stem cells. Cell. 1986;45:917-927.
26. Prosper F, Verfaillie CM. Regulation of hematopoiesis through adhesion receptors. J Leukoc Biol. 2001;69:307-316.
27. Lapidot T. Mechanism of human stem cell migration and repopulation of NOD/SCID and B2mnull NOD/SCID mice. The role of SDF-1/CXCR4 interactions. Ann N Y Acad Sci. 2001;938:83-95.
28. Peled A, Petit I, Kollet O, et al. Dependence of human stem cell engraftment and repopulation of NOD/SCID mice on CXCR4. Science. 1999;283: 845-848.
29. Peled A, Kollet O, Ponomaryov T, et al. The chemokine SDF-1 activates the integrins LFA-1, VLA-4, and VLA-5 on immature human CD34(+) cells: role in transendothelial/stromal migration and engraftment of NOD/SCID mice. Blood. 2000;95:3289-3296.
30. Bonnet D, Dick JE. Human acute myeloid leukemia is organized as a hierarchy that originates from a primitive hematopoietic cell. Nat Med. 1997;3:730-737.
31. Zhong JF, Zhan Y, Anderson WF, Zhao Y. Murine hematopoietic stem cell distribution and proliferation in ablated and nonablated bone marrow transplantation. Blood. 2002;100:3521-3526.
32. Kollet O, Spiegel A, Peled A, et al. Rapid and efficient homing of human CD34(+)CD38(-/low) CXCR4(+) stem and progenitor cells to the bone marrow and spleen of NOD/SCID and NOD/SCID/B2m(null) mice. Blood. 2001;97:3283-3291.
33. Papayannopoulou T, Craddock C, Nakamoto B, Priestley GV, Wolf NS. The VLA4/VCAM-1 adhesion pathway defines contrasting mechanisms of lodgement of transplanted murine hemopoietic progenitors between bone marrow and spleen. Proc Natl Acad Sci U S A. 1995;92:9647-9651.
34. Zanjani ED, Flake AW, Almeida-Porada G, Tran N, Papayannopoulou T. Homing of human cells in the fetal sheep model: modulation by antibodies activating or inhibiting very late activation antigen-4-dependent function. Blood. 1999;94: 2515-2522.
35. Verfaillie CM, McCarthy JB, McGlave PB. Differentiation of primitive human multipotent hematopoietic progenitors into single lineage clonogenic progenitors is accompanied by alterations in their interaction with fibronectin. J Exp Med. 1991;174: 693-703.
36. Teixido J, Hemler ME, Greenberger JS, Anklesaria P. Role of beta 1 and beta 2 integrins in the adhesion of human CD34hi stem cells to bone marrow stroma. J Clin Invest. 1992;90:358-367.
37. Simmons PJ, Masinovsky B, Longenecker BM, Berenson R, Torok-Storb B, Gallatin WM. Vascular cell adhesion molecule-1 expressed by bone

marrow stromal cells mediates the binding of hematopoietic progenitor cells. Blood. 1992;80: 388-395.

38. Sanz-Rodriguez F, Hidalgo A, Teixido J. Chemokine stromal cell-derived factor-1alpha modulates VLA-4 integrin-mediated multiple myeloma cell adhesion to CS-1/fibronectin and VCAM-1. Blood. 2001;97:346-351.
39. Hidalgo A, Sanz-Rodriguez F, Rodriguez-Fernandez JL, et al. Chemokine stromal cell-derived factor-1alpha modulates VLA-4 integrin-dependent adhesion to fibronectin and VCAM-1 on bone marrow hematopoietic progenitor cells. Exp Hematol. 2001;29:345-355.
40. Lataillade JJ, Clay D, Dupuy C, et al. Chemokine SDF-1 enhances circulating CD34(+) cell proliferation in synergy with cytokines: possible role in progenitor survival. Blood. 2000;95:756-768.
41. Cashman J, Clark-Lewis I, Eaves A, Eaves C. Stromal-derived factor 1 inhibits the cycling of very primitive human hematopoietic cells in vitro and in NOD/SCID mice. Blood. 2002;99: 792-799.
42. Lataillade JJ, Clay D, Bourin P, et al. Stromal cell-derived factor 1 regulates primitive hematopoiesis by suppressing apoptosis and by promoting G(0)/G(1) transition in CD34(+) cells: evidence for an autocrine/paracrine mechanism. Blood. 2002;99:1117-1129.
43. Glimm H, Tang P, Clark-Lewis I, von Kalle C, Eaves C. Ex vivo treatment of proliferating human cord blood stem cells with stroma-derived factor-1 enhances their ability to engraft NOD/SCID mice. Blood. 2002;99:3454-3457.
44. Bhatia M, Bonnet D, Murdoch B, Gan OI, Dick JE. A newly discovered class of human hematopoietic cells with SCID-repopulating activity. Nat Med. 1998;4:1038-1045.
45. Nakamura Y, Ando K, Chargui J, et al. Ex vivo generation of CD34(+) cells from CD34(-) hematopoietic cells. Blood. 1999;94:4053-4059.
46. Osawa M, Hanada K, Hamada H, Nakauchi H. Long-term lymphohematopoietic reconstitution by a single CD34-low/negative hematopoietic stem cell. Science. 1996;273:242-245.
47. Kushida T, Inaba M, Ikebukuro K, et al. Comparison of bone marrow cells harvested from various bones of cynomolgus monkeys at various ages by perfusion or aspiration methods: a preclinical study for human BMT. Stem Cells. 2002;20:155-162.

Journal of the American College of Cardiology
© 2003 by the American College of Cardiology Foundation
Published by Elsevier Science Inc.

Vol. 41, No. 6, 2003
ISSN 0735-1097/03/$30.00
doi:10.1016/S0735-1097(02)03007-3

Biodegradable Gelatin Hydrogel Potentiates the Angiogenic Effect of Fibroblast Growth Factor 4 Plasmid in Rabbit Hindlimb Ischemia

Hirofumi Kasahara, MD,* Etsuro Tanaka, MD, PHD,†§ Naoto Fukuyama, MD, PHD,†§ Eriko Sato, MD,* Hiromi Sakamoto, PHD,‖ Yasuhiko Tabata, PHD,¶ Kiyoshi Ando, MD, PHD,‡§ Harukazu Iseki, MD, PHD,‡ Yoshiro Shinozaki, BS,† Koji Kimura, MD,* Eriko Kuwabara, MD,* Shirosaku Koide, MD, PHD,* Hiroe Nakazawa, MD, PHD,† Hidezo Mori, MD, PHD#

Isehara, Tokyo, Kyoto, and Suita, Japan

OBJECTIVES We investigated the potentiation of gene therapy using fibroblast growth factor 4 (FGF4)-gene by combining plasmid deoxyribonucleic acid (DNA) with biodegradable gelatin hydrogel (GHG).

BACKGROUND Virus vectors transfer genes efficiently but are biohazardous, whereas naked DNA is safer but less efficient. Deoxyribonucleic acid charges negatively; GHG has a positively charged structure and is biodegradable and implantable; FGF4 has an angiogenic ability.

METHODS The GHG-DNA complex was injected into the hindlimb muscle (63 mice and 55 rabbits). Gene degradation was evaluated by using ^{125}I-labeled GHG-DNA complex in mice. Transfection efficiency was evaluated with reverse-transcription nested polymerase chain reaction and X-Gal histostaining. The therapeutic effects of GHG-FGF4-gene complex (GHG-FGF4) were evaluated in rabbits with hindlimb ischemia.

RESULTS Gelatin hydrogel maintained plasmid in its structure, extending gene degradation temporally until 28 days after intramuscular delivery, and improving transfection efficiency. Four weeks after gene transfer, hindlimb muscle necrosis was ameliorated more markedly in the GHG-FGF4 group than in the naked FGF4-gene and GHG-beta-galactosidase (control) groups ($p < 0.05$, Kruskal-Wallis test). Synchrotron radiation microangiography (spatial resolution, 20 μm) and flow determination with microspheres confirmed significant vascular responsiveness to adenosine administration in the GHG-FGF4 group, but not in the naked FGF4-gene and the control.

CONCLUSIONS The GHG-FGF4 complex promoted angiogenesis and blood flow regulation of the newly developed vessels possibly by extending gene degradation and improving transfection efficiency without the biohazard associated with viral vectors. (J Am Coll Cardiol 2003;41: 1056–62) © 2003 by the American College of Cardiology Foundation

Angiogenic gene therapy using growth factors is widely studied to treat ischemic heart disease and severe limb ischemia (1,2). Of the two major methods of gene transfer, the use of virus vectors is efficient but biohazardous (3,4), while naked deoxyribonucleic acid (DNA) is safer, but less efficient (5). A highly efficient and safe drug delivery system without using a virus vector is needed for gene therapy in humans. We developed a new hydrogel consisting of amino acids, being biodegradable and, therefore, implantable, from gelatin (6). Hydrogel has been used to improve transfection efficiency in a hydrogel-coated balloon catheter (7). However, this hydrogel was not implantable because it consisted of carbohydrate and was not biodegradable. The purpose of the present study is to assess whether biodegradable gelatin hydrogel (GHG) improves the efficacy of gene therapy with the fibroblast growth factor 4 (FGF4)/hst1 gene; FGF4 is a growth factor discovered in human gastric cancer (8) and has a secretion signal domain (9). Its angiogenic ability has been confirmed both in vitro and in vivo (10).

METHODS

Experimental animals. All animal experiments were performed in accordance under the Guidelines of Tokai University School of Medicine on Animal Use, which conform to the National Institute of Health (NIH) Guide for the Care and Use of Laboratory Animals, DHEW publication No. (NIH) 86-23, revised 1985, Offices of Science and Health Reports, DRR/NIH, Bethesda, Maryland. Fifty-five Japanese white rabbits weighting 2.45 to 2.85 kg (Nihon Nosan Co., Tokyo, Japan) of both genders were used. The animals were anesthetized by intravenous injection of sodium pentobarbital (40 mg/kg), and hindlimb ischemia was created by the method of Takeshita et al. (11). Sixty-three

From the Departments of *Cardiovascular Surgery, †Physiology, ‡Internal Medicine, and §Research Center for Genetic Engineering and Cell Transplantation, Tokai University School of Medicine, Isehara, Japan; ‖Genetics Division, National Cancer Center Research Institute, Tokyo, Japan; ¶Research Center for Biomedical Engineering, Kyoto University, Kyoto, Japan; #Department of Cardiac Physiology, National Cardiovascular Center Research Institute, Suita, Japan. Supported by Grants-in-Aid for Scientific Research (13470154, 13470381, 13877114, 14657460, 14657461) from the MECSST; New Energy and Industrial Technology Development Organization; The Science Frontier Program of MESSC; The Research Grants for Cardiovascular Disease (H13C-1) and for Cancer Research (9-3, 10Shi-1) from the MHLW; HLSRG-H14nano001&genom005; the Promotion of Fundamental Studies in Health Science of the Organization for Pharmaceutical Safety and Research of Japan.

Manuscript received December 30, 2001; revised manuscript received July 2, 2002, accepted November 5, 2002.

Abbreviations and Acronyms

ANOVA	= analysis of variance
cDNA	= complementary deoxyribonucleic acid
DNA	= deoxyribonucleic acid
FGF4	= fibroblast growth factor 4
GHG	= gelatin hydrogel
lacZ	= beta-galactosidase
NIH	= National Institute of Health
PBS	= phosphate-buffered saline
pI	= isoelectric point
RNA	= ribonucleic acid
RT-nested PCR	= reverse transcription-nested polymerase chain reaction

mice (male ddY mice, six to seven weeks old, Shizuoka Animal Center, Shizuoka, Japan) were also used.

Preparation of GHG-DNA complex. DNA encoding FGF4, beta-galactosidase (lacZ) with the cytomegalovirus enhancer-chicken β-actin hybrid promoter comprising a cytomegalovirus enhancer, and chicken beta-actin promoter were constructed (12); GHG was prepared from bovine bone (6). The GHG used in this study was characterized by a spheroid shape with a diameter of approximately 200 μm, water content of 95%, and an isoelectric point (pI) of 11 after swelling in water, without special statement.

The efficiency of incorporation of DNA into positively and negatively charged GHG was evaluated. Dried GHG (4 mg, pI 11 or 5) was added to lacZ DNA solution (500 μg/100 μl in phosphate-buffered saline [PBS], pH 7.4), mixed with a vortex mixer for 5 s, and allowed to stand at 37°C; the solution immediately settled. The absorbance (260 nm) of the supernatant was measured. In a sham control experiment, GHG was added to pure PBS solution. Positively charged GHG (pI 11) was immediately impregnated with naked DNA, and was stable at pH 7.4 for at least 120 h, whereas the negatively charged one (pI 5) was not.

Experimental protocols. PROTOCOL 1: DNA DEGRADATION AND THE IMPROVEMENT OF TRANSFECTION EFFICIENCY BY GHG. To examine the temporal extension of gene degradation by GHG, the decay sequence of ^{125}I-labeled DNA impregnated into unlabeled GHG, ^{125}I-labeled GHG, and ^{125}I-labeled DNA solution was compared (63 mice). Plasmid DNA and GHG were radioiodinated with ^{125}I, with TlCl3 and Bolton and Hunter reagent (Amersham Pharmacia Biotech Ltd., Buckinghamshire, United Kingdom) (13), respectively. To impregnate GHG with DNA, dried GHG (2 mg) was added to 100 μl of naked lacZ solution (50 μg/100 μl in PBS), mixed for 5 s, and allowed to stand at 37°C for 2 h. Each complex was injected into the hindlimb muscle. On days 1, 3, 5, 7, 14, 21, or 28, the muscle was collected, and radioactivity was measured with a gamma counter (ARC-301B, Aloka Co., Ltd., Tokyo, Japan) in three mice each.

The following experiment was performed in 16 rabbits to assess spatial potentiation of gene expression by GHG. Intramuscular gene transfer was performed 10 days after modeling hindlimb ischemia. The DNA solution (FGF4-gene or lacZ 500 μg/100 μl PBS) mixed with GHG (4 mg; GHG-FGF4 complex, n = 2; GHG-lacZ complex, n = 2) and the original FGF4-gene solution (naked FGF4-gene, n = 2) were diluted with 0.4 ml saline and slowly injected through a 23-gauge needle at a single point in the adductor muscle marked with a 4-0 nylon suture. Tissue samples from the transfected left adductor muscle (the injection site and the adjacent region 10 mm apart from the injection site), the right adductor muscle, stomach, liver, spleen, testes, kidneys, heart, lungs, and brain were retrieved and immediately frozen in liquid nitrogen on day 17; FGF4-gene expression was evaluated by reverse transcription-nested polymerase chain reaction (RT-nested PCR). In the remaining 10 rabbits, gene expression was evaluated with lacZ gene; GHG-lacZ complex (n = 5) and naked lacZ solution (n = 5) were injected at a single point in the adductor muscle in the same way as the GHG-FGF4 injection on day 10. On day 17, a muscle sample at the injection site was dissected out, and expression of lacZ was determined by X-Gal histostaining (14).

PROTOCOL 2: SALVAGE OF HINDLIMB ISCHEMIA WITH GHG-PLASMID COMPLEX ENCODING FGF4. The angiogenic effect of three sets of GHG-DNA complexes were compared in 39 rabbits with hindlimb ischemia: 1) GHG impregnated with lacZ plasmid (GHG-lacZ: control); 2) naked FGF4-plasmid (naked FGF4-gene); and 3) GHG impregnated with FGF4 plasmid (GHG-FGF4). The amount of plasmid was 500 μg (1.0 ml) and that of GHG was 4 mg. On day 10 of ischemia, the gene complex was injected at five points 20 mm apart in the adductor muscle with a 23-gauge needle.

In 18 rabbits, on days 10 and 38 of ischemia, calf systolic blood pressure was measured by the Doppler flow signal from the posterior tibial artery (ES-100V2, Hayashi Denki Co., Kawasaki, Japan) with a 25-mm wide cuff. The calf blood pressure ratio of each rabbit was defined as the ratio of the systolic pressure of the ischemic limb to that of the normal limb. Regional blood flow was measured by the microsphere method (15) at baseline on days 0 and 38. On day 38, adenosine (100 μg/kg/min) was administered 30 min after baseline flow measurement (vasodilatory condition). A 4F catheter was introduced into the ascending aorta via the common carotid artery for microsphere injection and adenosine administration. Microspheres (15-μm diameter, 3 × 106) labeled with one of four sets of stable heavy elements (In, I, Ba, or Ce, Sekisui Plastic, Osaka, Japan) (15) were suspended in 0.05% sodium dodecyl sulfate at a concentration of 5 × 106/ml and injected into the ascending aorta. After killing the animals, the adductor, semimembranous, and gastrocnemius muscles were dissected out and weighed. The X-ray fluorescence of the labeled microspheres was measured in 4 to 8 g of the dissected muscles to calculate the regional blood flow (15) and expressed as the ratio of flow in the ischemic limb to flow in the normal limb.

JACC Vol. 41, No. 6, 2003
March 19, 2003:1056–62

Table 1. Morphologic Evaluation of Gene Therapy

Muscle Necrosis (Area)	GHG-lacZ	Naked FGF4	GHG-FGF4*†
Grade 0 (0 cm^2)	0	0	0
Grade 1 (<1 cm^2)	0	0	50% (3/6)
Grade 2 (<3 cm^2)	17% (1/6)	33% (2/6)	50% (3/6)
Grade 3 (<5 cm^2)	0	67% (4/6)	0
Grade 4 (<10 cm^2)	50% (3/6)	0	0
Grade 5 (>10 cm^2)	33% (2/6)	0	0
Muscle weight ratio (%)	48 ± 67 (6)	62 ± 14 (6)	79 ± 11* (6)

Morphologic indexes in 18 gene-transferred rabbits on day 38. The ischemic limb was macroscopically evaluated by using graded morphological scales for muscle necrosis area (the adductor, semimembranous, medial large, and gastrocnemius muscles) (grade 0 to 5); GHG-FGF4 group had significantly less muscle necrosis compared with naked FGF4 and GHG-lacZ groups. Muscle weight ratio was significantly different between GHG-FGF4 and GHG-lacZ groups. $p < 0.05$ vs. *GHG-lacZ, †naked FGF4 (Kruskal-Wallis test, analysis of variance).

FGF4 = fibroblast growth factor 4; GHG = gelatin hydrogel; lacZ = β-galactosidase.

Sufficient mixing of microspheres injected into the aorta (not into the left atrium) was confirmed by a preliminary study in which two different sets of microspheres were simultaneously injected into the aorta. The liner regression analysis on the two different sets of flows yielded an almost identical regression line ($y = 1.011x - 0.003$, $r = 0.98$, $Sy \cdot \hat{x} = 0.032$). The remaining muscle tissue was used for histological analysis. An investigator blinded to the treatment macroscopically evaluated the ischemic limb on graded morphological scales for area of muscle necrosis (the adductor, semimembranous, medial large, and gastrocnemius muscles; grade 0 to 5; Table 1).

Synchrotron radiation microangiography characterized by high-resolution and high-sensitivity (16) was performed in 21 rabbits as previously described (15,17,18). The system is capable of separating adjacent lead lines only 20 μm apart on the resolution bar chart with 640× higher sensitivity than charge-coupled device camera system. This system allows detection and functional analysis of small vessels with a diameter of 200 to 500 μm in situ (15,17,18). Contrast material containing 37% nonionic iodine (Iopamidol, Nihon Schering Co., Tokyo, Japan) was injected via a 4F catheter placed immediately above the aortic bifurcation under baseline condition and during adenosine administration (100 μg/kg/min) (vasodilatory condition) via the same catheter. Vessel density in the midzone collateral was evaluated as an angiographic score (11,15,18).

Plasmid. Complementary deoxyribonucleic acid (cDNA) of human hst1/FGF4 (19), or bacterial β-galactosidase was inserted into the expression vector pRC/CMV (Invitrogen Corp., Carlsbad, California) and designated as pRC/CMV-HST1-10 (human stomach tumor) and pRC/CMV-lacZ, respectively. Preparation and purification of the plasmid from cultures of pRC/CMV-HST1-10-, or pRC/CMV-lacZ-transformed *Escherichia coli* were performed by centrifugation to equilibrium in cesium chloride-ethidium bromide gradients.

RT-nested PCR. Ribonucleic acid (RNA) was extracted from tissues with ISOGEN (Nippon Gene, Tokyo, Japan). The extracted RNA was treated with DNase twice to eliminate DNA contamination. In each set of experiments, 0.5 μg of total RNA was denatured at 70°C for 5 min, and reverse transcription was carried out at 37°C for 60 min; RT-nested PCR was carried out in a thermal cycler (GeneAmp PCR System 9600, Perkin Elmer, Wellesley, Massachusetts) with primers designed to selectively amplify the FGF4 cDNA. The external primers EcoHST1f3 (forward primer: GGA ATT CAC TGA CCG CCT GAC CGA CGC ACG GCC CTC G) and SalHST1r2 (reverse primer: GCG TCG ACC CCG AGG CTG AGG CAA GGG TCC TCT) were used for the first round (generating a 704-base pair [bp] fragment). The second round of the amplification (nested PCR) was performed with two internal primers HST1LGC1 (forward primer: AGC TCT CGC CCG TGG AGC GG) and HST1AA-r (reverse primer: CTC TGG AGG GTC ACA GCC TG) (generating a 282-bp fragment). The PCR reactions were performed as follows. The thermal cycle conditions for the first round were 30 cycles (95°C for 1 min, 59°C for 1 min, 72°C for 1 min), and for the second round were 25 cycles (94°C for 1 min, 72°C for 2 min), followed by incubation at 72°C for 10 min, respectively. Amplification products were detected after electrophoresis on 3.5% agarose gels by staining with ethidium bromide. A primer set of beta-actin (generating a 506-bp fragment) was used as a positive control for RT-PCR analysis.

Statistical analysis. Data are presented as mean values ± SD. Differences were assessed by using the paired *t* test, Kruskal-Wallis test, or analysis of variance (ANOVA) for factorial or repeated measures with the Scheffé F test when applicable. A value of $p < 0.05$ was considered statistically significant.

RESULTS

Protocol 1: DNA degradation and the improvement of transfection efficiency by GHG. The radioactivity of radiolabeled DNA impregnated into GHG in the limb muscle remained above the detection limit for four weeks (solid line in Fig. 1). The radiolabeled DNA impregnated into GHG had decay sequences almost identical to those of the radiolabeled GHG (dotted line in Fig. 1). By contrast, the radioactivity of naked DNA (dashed line in Fig. 1) decreased to <10% of the baseline within a day.

Gelatin hydrogel improved transfection efficiency in vivo; RT nested-PCR analyses revealed FGF4 expression at all injection sites in the left adductor muscle in the FGF4-gene-treated animals (n = 4), as shown in lanes 1 (naked FGF4-gene) and 4 (GHG-FGF4) in Figure 2; FGF4 expression was also detected in the adjacent region 10 mm apart from the injection site in the left adductor muscle in the GHG-FGF4-treated animals (lane 5), but not in the naked FGF4-gene-treated animals (lane 2). No expression was detected in any animal at remote sites, such as the right adductor muscle (lanes 3 and 6), stomach, liver, spleen,

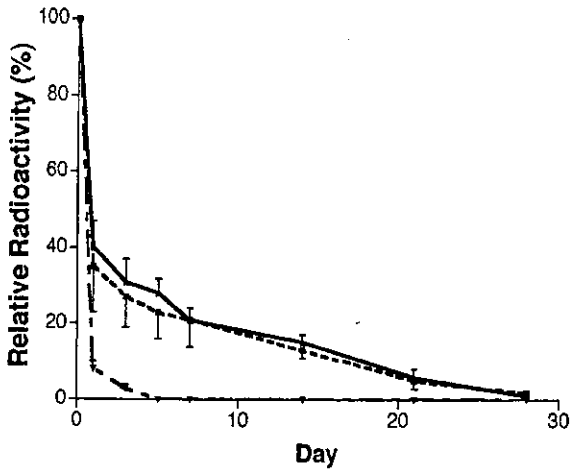

Figure 1. Decay sequences of radiolabeled deoxyribonucleic acid (DNA), gelatin hydrogel (GHG), and DNA combined with GHG in the hindlimb muscles of mice. Unlabeled GHG impregnated with ^{125}I-labeled DNA **(solid line)**, ^{125}I-labeled GHG **(dashed line)**, and ^{125}I-labeled DNA solution **(dotted line)** were injected into the hindlimb muscles.

testes, kidneys, heart, lungs, or brain (data not shown); lacZ-treated animals showed no FGF4 expression at any sites (lanes 7 and 8). Beta-actin expression was detected in all samples (lower panel), but neither beta-actin nor FGF4 expression was detected in any control samples that were not treated with reverse transcriptase; lacZ expression of naked DNA (500 μg) was localized to the injection site (Fig. 3A), whereas GHG-DNA complex (DNA amount 500 μg) showed a spatially expanded expression on day 17 (Fig. 3B). The degree of gene expression in myocytes was also augmented by GHG.

Protocol 2: salvage of hindlimb ischemia with GHG-plasmid complex encoding FGF4. Functional evaluation of ischemic hindlimbs showed amelioration of the ischemia

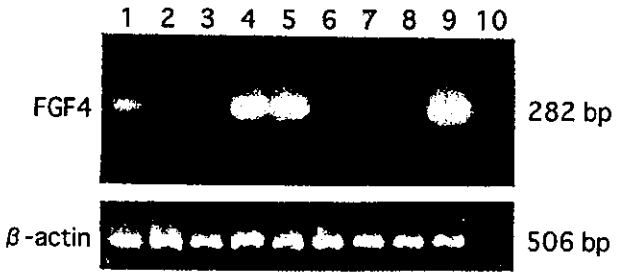

Figure 2. Representative transgene expression demonstrated by reverse-transcription nested polymerase chain reaction (RT-nested PCR). The left adductor muscle of the rabbits was injected with naked fibroblast growth factor 4 (FGF4) gene **(lanes 1 to 3)**, gelatin hydrogel (GHG)-FGF4 **(lanes 4 to 6)**, or GHG-lacZ **(lanes 7 and 8)**. Each sample was obtained from the injection site **(lanes 1, 4, and 7)** and the adjacent region 10 mm apart from the injection site **(lanes 2, 5 and 8)** in the left adductor muscle, and from the contralateral adductor muscle **(lanes 3 and 6)**. The RT-nested PCR products from ribonucleic acid of each sample were analyzed on agarose gel; FGF4 expressed Cc1/l6 cells as a positive control **(lane 9)** and no deoxyribonucleic acid (DNA) template as a negative control **(lane 10)**. A housekeeping beta-actin gene was amplified as a complementary DNA loading control.

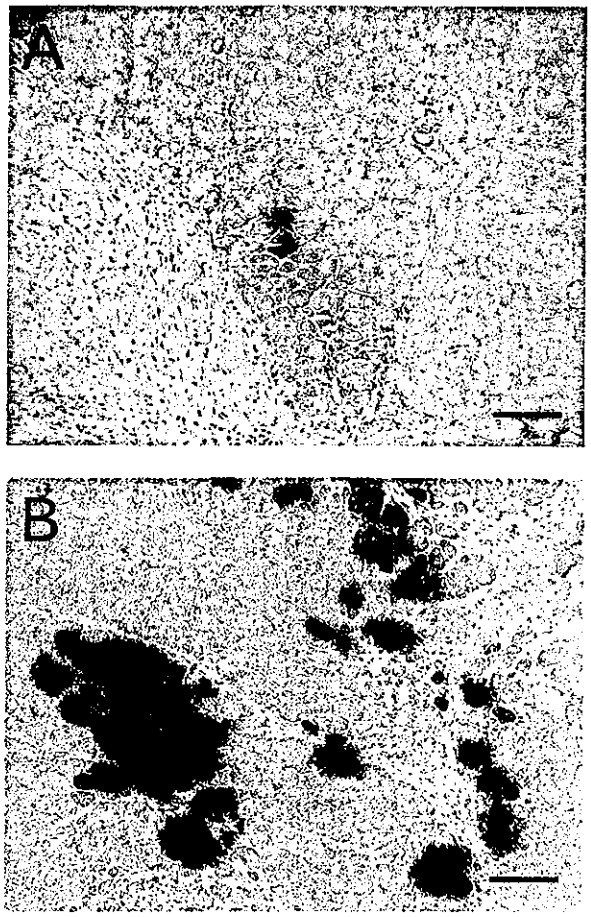

Figure 3. Representative gene expression of lacZ in the ischemic adductor muscle in rabbits on day 17. Naked deoxyribonucleic acid (DNA) **(A)** or gelatin hydrogel-DNA complex **(B)** was injected into the adductor muscle 10 days after the ischemic insult. X-Gal stain; original magnification ×20; bar = 200 μm.

by the FGF4-gene and potentiation of the amelioration when GHG was used as a delivery device. The augmentation of regional blood flow with GHG was more evident under vasodilatory conditions than at the baseline.

Regional blood flow analysis and angiographic analysis further confirmed the background mechanism for amelioration of hindlimb ischemia by GHG-FGF4 (Table 2). On day 38, blood flow during adenosine administration (vasodilatory condition) in the GHG-FGF4 group (105 ± 13% in terms of ischemic/normal flow ratio) was significantly higher than in either the naked FGF4-gene group (68 ± 18%, $p < 0.05$) or the GHG-lacZ group (50 ± 12%, $p < 0.05$, ANOVA). The differences between the naked FGF4-gene and GHG-lacZ groups were not significant (ANOVA). The adenosine-dependent flow-augmentation (responsiveness to vasodilatory stimulation; comparison between adenosine and baseline values on day 38) was noted only in the GHG-FGF4 group (from 79 ± 16% to 105 ± 13%, $p < 0.05$, ANOVA), and not in the other two groups. A similar tendency was noted in flow under baseline conditions on day 38 in all three groups; however, the

JACC Vol. 41, No. 6, 2003
March 19, 2003:1056–62

Table 2. Functional Evaluation of Gene Therapy

	GHG-lacZ	Naked FGF4	GHG-FGF4
Blood flow ratio (%) (ischemic/normal)			
Day 0 (BL)	33 ± 8 (6)	36 ± 11 (6)	37 ± 10 (6)
Day 38 (BL)	47 ± 12‡ (6)	58 ± 16‡ (6)	79 ± 16*‡ (6)
Day 38 (Ad)	50 ± 12‡ (6)	68 ± 18‡ (6)	105 ± 13*†‡§ (6)
Angiographic score			
Day 38 (BL)	0.37 ± 0.12 (7)	0.39 ± 0.13 (7)	0.42 ± 0.11 (7)
Day 38 (Ad)	0.36 ± 0.10 (7)	0.41 ± 0.13 (7)	0.56 ± 0.15*†§ (7)
Blood pressure (%) (ischemic/normal)			
Day 10	31 ± 8 (6)	33 ± 5 (6)	26 ± 7 (6)
Day 38	56 ± 4 (6)	63 ± 6 (6)	70 ± 11* (6)

Angiographic score was calculated on the synchrotron radiation microangiogram. $p < 0.05$ vs. *GHG-lacZ, †naked FGF4, ‡day 0 (BL), and §day 38 (BL) (analysis of variance).

Ad = during adenosine administration; BL = under baseline condition; FGF4 = fibroblast growth factor 4; GHG = gelatin hydrogel; lacZ = β-galactosidase.

differences in baseline flow among the three groups were less marked than during adenosine administration.

Synchrotron radiation microangiography revealed microvessel responsiveness to the vasodilatory stimulation in the GHG-FGF4-treated rabbits (Figs. 4C and 4D), whereas vascular density was somewhat decreased by adenosine treatment in some of the GHG-lacZ-treated rabbits (Figs. 4A and 4B). Angiographic score analysis yielded quantitative evidence (Table 2). The angiographic score during adenosine administration (vasodilatory condition) was significantly higher in the GHG-FGF4 group (0.56 ± 0.15) than in either the naked FGF4-gene group (0.41 ± 0.13, $p < 0.05$) or the GHG-lacZ group (0.36 ± 0.10, $p < 0.05$, ANOVA). By contrast, under baseline conditions, the angiographic scores of the three groups were not significantly different.

On day 38, the GHG-FGF4 group had the highest calf-blood pressure ratio (70 ± 11%), and it was lower in the naked FGF4-gene group (63 ± 6%), and even lower in the GHG-lacZ group (56 ± 4%, $p < 0.05$ vs. the GHG-lacZ group, ANOVA, Table 2). On day 10 (the time of gene transfer), the degrees of decrease in the three groups were not significantly different (26% to 33% in the mean).

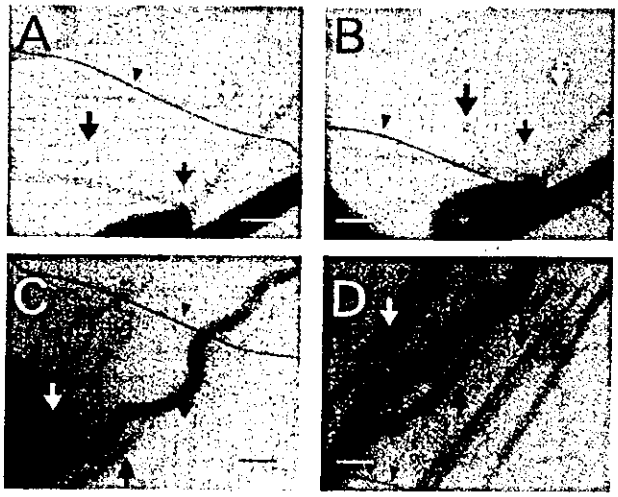

Figure 4. Representative synchrotron radiation microangiograms of the hindlimb ischemia in the rabbits. Synchrotron radiation microangiograms were taken under baseline conditions **(A and C)** and after repeated adenosine administration **(B and D)** on day 38. **(A and B)** Gelatin hydrogel (GHG)-lacZ-treated rabbit; **(C and D)** GHG-fibroblast growth factor 4-treated rabbit. **Arrows** indicate the same point in the vessels. **Arrowheads** reference copper wires with a diameter of 130 μm; **bar** = 1 mm.

Tissue damage was least in the GHG-FGF4-treated rabbits (Table 1). Limb muscle necrosis was <3 cm^2 and grade 1 or 2 in all of the animals in the GHG-FGF4 group, and significantly less than in the other two groups ($p < 0.05$, Kruskal-Wallis test). A similar difference was noted in the degrees of toe necrosis (data not shown). The muscle weight ratio (ischemic/normal) on day 38 was highest in the GHG-FGF4 group (79 ± 11%), lower in the naked FGF4-gene group (62 ± 14%), and even lower in the GHG-lacZ group (48 ± 67%), and the difference between the GHG-FGF4 group and GHG-lacZ group was significant ($p < 0.05$, ANOVA). The muscle weight ratio values (a morphological index) positively correlated with vascular responsiveness to adenosine (adenosine/baseline blood flow ratio [%]; a functional index) ($r = 0.50$, $n = 18$, $Sy \cdot x = 0.15$, $Sy \cdot x/y = 0.23$, $p = 0.045$). Thus, the blood flow, microangiographic, and morphologic analyses demonstrated a greater ameliorative effect of the GHG-FGF4 complex compared with the naked FGF4-gene (Tables 1 and 2).

Minimal inflammatory infiltrates, such as neutrophil and lymphoplasmacytic cell infiltrates, were noted at the injection site, but histological analysis showed that the infiltrates were localized. There was no evidence of fibrous proliferation or tumor formation in the transfected muscles or in other organs (right adductor muscle, stomach, liver, spleen, testes, kidneys, heart, lungs, and brain) in any of the groups.

DISCUSSION

We demonstrated that GHG potentiated the angiogenic effect of the FGF4-gene (protocol 2) by prolonging DNA degradation and improving transfection efficiency (protocol 1). Thus, GHG might facilitate the gene therapy of intractable circulatory disorders with genes for angiogenic growth factors.

Gelatin hydrogel augmented the effect of the FGF4-gene

therapy by improving gene biodegradation and transfection efficiency. We demonstrated that GHG rapidly absorbed plasmid DNA and did not release it in vitro (see Methods section). In the radioiodine experiment, the radioactivity of naked DNA was reduced to less than 10% of the baseline within a day, whereas the radioactivity of DNA impregnated into GHG remained for four weeks (Fig. 1). In the experiment using the rabbit hindlimb ischemia model, the PCR analysis suggested that GHG expanded the gene transfer spatially (lanes 2 and 5 in Fig. 2). The maker gene experiment (protocol 1) confirmed that the use of GHG augmented both the number of transfected myocytes and the degree of gene expression in these cells, and also supported the spatially expanded gene expression (Fig. 3). The superiority of the therapeutic effects of the GHG-FGF4-gene complex on hindlimb ischemia compared with naked FGF4-gene treatment was confirmed in the rabbit experiments in protocol 2 (Fig. 4, Tables 1 and 2); GHG-FGF4-treated rabbits were characterized by less severe tissue damage in the ischemic limb (Table 2) and more marked vascular responsiveness to adenosine than either the naked FGF4-treated or GHG-lacZ-treated rabbits (Fig. 4, Table 2, Protocol 2 in the Results section). Under the baseline conditions, blood flow in normal muscle tissue is set at a relatively low level in preparation for an abrupt increase in flow demand (approximately 5× and 30× in the heart and in the skeletal muscle, respectively) during exercise, etc. (responsiveness to the vasodilatory stimulation). In other words, normal muscle tissue has a sufficient flow reserve (20,21); and, thus, the presence or absence of vascular responsiveness to adenosine administration can be used as an index of fundamental vascular function in angiogenic vascular segments. The demonstration of a positive correlation between flow responsiveness to adenosine and the muscle weight ratio further supports our hypothesis. Baseline flow may reflect the total number of angiogenic vessels, if it does not respond to vasodilatory stimulation. However, if the vasodilatory mechanism is present, baseline flow alone does not necessarily reflect the quality and/or quantity of angiogenic vascular segments. The amelioration of the ischemic tissue in the GHG-FGF4 group may be related to an adequate flow reserve (20,21) of so-called "well-tempered angiogenic vessels" (22).

Consequently, GHG offers several advantages as a new gene delivery system: 1) it has a positively charged structure, so it holds negatively charged nucleic acids, proteins, and drugs within its structure; 2) GHG is biodegradable and implantable; the biodegradable nature is from the gelatin itself but not from the hydrogel state. The substance bound to the GHG is gradually released as the gelatin degrades in situ. The degradation period can be adjusted to two to four weeks by varying the water content. Thus, the prolonged release of the DNA held in GHG was presumably responsible for the augmentation of gene therapy. The use of hydrogel-coated balloon-angioplasty-catheter has been reported (7). However, this gel is much different from our hydrogel. The present GHG consists of amino acids and is biodegradable and implantable, whereas their hydrogel consists of carbohydrate and is not biodegradable nor implantable. 3) The isoelectric point and the shape of the GHG can be modified. Negatively charged GHG holds positively charged substances such as basic-FGF protein (6,23), and disk-shaped GHG has been found to be effective for reconstruction of bone defects (23); 4) GHG is less biohazardous than adenovirus vectors. Gelatin is already used in the clinical field, and its safety is established. Thus, the use of GHG with naked DNA improves its transfection efficiency without causing serious cytotoxicity or biohazards, which are inconvenient side effects of virus vectors (24). Therefore, the nonvirus vector GHG is useful for various gene therapies including the treatment of cardiovascular disorders.

Acknowledgments

The authors wish to thank Chiharu Tada, Akiko Hori, Sachie Ueno, and Takayuki Hasegawa for their technical work.

Reprint requests and correspondence: Dr. Hidezo Mori, Department of Cardiac Physiology, National Cardiovascular Center Research Institute, 5-7-1 Fujishirodai, Suita 565-8565, Japan. E-mail: hidemori@ri.ncvc.go.jp.

REFERENCES

1. Asahara T, Bauters C, Zheng LP, et al. Synergistic effect of vascular endothelial growth factor and basic fibroblast growth factor on angiogenesis in vivo. Circulation 1995;92:417–27.
2. Aoki M, Morishita R, Taniyama Y, et al. Angiogenesis induced by hepatocyte growth factor in non-infarcted myocardium and infarcted myocardium: up-regulation of essential transcription factor for angiogenesis. Gene Ther 2000;7:417–27.
3. Yang Y, Trinchieri G, Wilson JM. Recombinant IL-12 prevents formation of blocking IgA antibodies to recombinant adenovirus and allows repeated gene therapy to mouse lung. Nat Med 1995;1:890–3.
4. Zabner J, Ramsey BW, Meeker DP, et al. Repeat administration of an adenovirus vector encoding cystic fibrosis transmembrane conductance regulator to the nasal epithelium of patients with cystic fibrosis. J Clin Invest 1996;97:1504–11.
5. Takeshita S, Isshiki T, Sato T. Increased expression of direct gene transfer into skeletal muscles observed after acute ischemic injury in rats. Lab Invest 1996;74:1061–5.
6. Tabata Y, Hijikata S, Muniruzzaman M, Ikada Y. Neovascularization effect of biodegradable gelatin microspheres incorporating basic fibroblast growth factor. J Biomater Sci Polym Ed 1999;10:79–94.
7. Isner JM, Pieczek A, Schainfeld R, et al. Clinical evidence of angiogenesis after arterial gene transfer of phVEGF165 in patients with ischaemic limb. Lancet 1996;348:370–4.
8. Sakamoto H, Mori M, Taira M, et al. Transforming gene from human stomach cancers and a noncancerous portion of stomach mucosa. Proc Natl Acad Sci USA 1986;83:3997–4001.
9. Fuller PF, Peters G, Dickson C. Cell transformation by kFGF requires secretion but not glycosylation. J Cell Biol 1991;115:547–55.
10. Yoshida T, Ishimaru K, Sakamoto H, et al. Angiogenic activity of the recombinant hst-1 protein. Cancer Lett 1994;83:261–8.
11. Takeshita S, Zheng LP, Brogi E, et al. Therapeutic angiogenesis: a single intra-arterial bolus of vascular endothelial growth factor augments revascularization in a rabbit ischemic hind limb model. J Clin Invest 1994;93:662–70.
12. Miyazaki J, Takaki S, Araki K, et al. Expression vector system based on the chicken beta-actin promoter directs efficient production of interleukin-5. Gene 1989;79:269–77.

13. Bolton AE, Hunter WM. The labelling of proteins to high specific radioactivities by conjugation to a ^{125}I-containing acylating agent. Biochem J 1973;133:529–39.
14. Ueno H, Li JJ, Tomita H, et al. Quantitative analysis of repeat adenovirus-mediated gene transfer into injured canine femoral arteries. Arterioscler Thromb Vasc Biol 1995;15:2246–53.
15. Tanaka E, Hattan N, Ando K, et al. Amelioration of microvascular myocardial ischemia by gene transfer of vascular endothelial growth factor in rabbits. J Thorac Cardiovasc Surg 2000;120:720–8.
16. Tanioka K, Yamazaki J, Shidara K, et al. Avalanche-mode amorphous selenium photoconductive target for camera tube. Adv Electronics Electron Phys 1988;74:379–87.
17. Mori H, Hyodo K, Tanaka E, et al. Small-vessel radiography in situ with monochromatic synchrotron radiation. Radiology 1996;201:173–7.
18. Takeshita S, Isshiki T, Ochiai M, et al. Endothelium-dependent relaxation of collateral microvessels after intramuscular gene transfer of vascular endothelial growth factor in a rat model of hindlimb ischemia. Circulation 1998;98:1261–3.
19. Taira M, Yoshida T, Miyagawa K, Sakamoto H, Terada M, Sugimura T. cDNA sequence of human transforming gene hst and identification of the coding sequence required for transforming activity. Proc Natl Acad Sci USA 1987;84:2980–4.
20. Austin RJ, Aldea GS, Coggins DL, Flynn AE, Hoffman JI. Profound spatial heterogeneity of coronary reserve: discordance between patterns of resting and maximal myocardial blood flow. Circ Res 1990;67:319–31.
21. Coggins DL, Flynn AE, Austin RJ, et al. Nonuniform loss of regional flow reserve during myocardial ischemia in dogs. Circ Res 1990;67:253–64.
22. Blau H, Banfi A. The well-tempered vessel. Nat Med 2001;7:532–4.
23. Yamada K, Tabata Y, Yamamoto K, et al. Potential efficacy of basic fibroblast growth factor incorporated in biodegradable hydrogels for skull bone regeneration. J Neurosurg 1997;86:871–5.
24. Marshall E. Gene therapy death prompts review of adenovirus vector. Science 1999;286:2244–5.

Bone Marrow Transplantation (2003) 32, 391–398

www.nature.com/bmt

Myeloid Reconstitution

Serum stem cell growth factor for monitoring hematopoietic recovery following stem cell transplantation

C Ito[1], H Sato[2], K Ando[1], S Watanabe[1], F Yoshiba[1], K Kishi[1], A Furuya[2], K Shitara[2], S Sugimoto[2], H Kohno[3], A Hiraoka[4] and T Hotta[1]

[1]*Department of Hematology, Oncology and Rheumatology, Tokai University School of Medicine, Kanagawa, Japan;* [2]*Tokyo Research Laboratories, Kyowa Hakko Kogyo Co., LTD., Tokyo Japan;* [3]*Kyowa Medex Co., LTD., Tokyo Japan; and* [4]*Department of Internal Medicine, Osaka Dental University, Osaka, Japan*

Summary:

Stem cell growth factor (SCGF) is a novel cytokine for primitive hematopoietic progenitor cells. Although it has burst-promoting activity and granulocyte/macrophage colony-promoting activity *in vitro*, its significance in hematopoiesis *in vivo* has not been elucidated. In this study, we have established enzyme-linked immunosorbent assay (ELISA) to quantify human SCGF and measured serum cytokines in normal volunteers and 27 patients undergoing stem cell transplantation (SCT), including six autologous and 21 allogeneic transplants. SCGF levels gradually increased after SCT regardless of graft-versus-host disease or type of transplant. The maximum level of SCGF was observed during the rapid granulocyte recovery phase in patients subjected to an autologous transplantation, and during the granulocyte stabilization phase in allogeneic patients. SCGF levels in PBSCT patients began to rise earlier than in BMT patients. Two patients with no increment of SCGF after SCT showed delayed engraftment. The source of SCGF was further analyzed by RT-PCR and we found that SCGF was highly expressed in bone marrow (BM) $CD34^+$ and $CD34^-CD33^+$ cells, but not in BM $CD34^-CD33^-$ cells, BM stromal cells and peripheral blood cells. The cell population expressing SCGF in BM possess the colony-forming cell activity. Therefore, serum SCGF can be an indicator of hematopoietic recovery following SCT.
Bone Marrow Transplantation (2003) **32**, 391–398. doi:10.1038/sj.bmt.1704152
Keywords: stem cell growth factor; hematopoiesis; stem cell transplantation; cytokines; indicator

We have previously identified a novel hematopoietic growth factor, the stem cell growth factor (SCGF).[1] It was detected in the cultured supernatant of KPB-M15 cells, a human myeloid cell line established from a patient with chronic myeloid leukemia in blast crisis.[2] The cDNA for SCGF encodes a 29-kDa polypeptide without N-linked glycosylation, which belongs to the C-type lectin superfamily. Its gene is located on chromosome 19 at position q13.3, where genes for early-acting hematopoietic growth factors of the *flk-2/flt3* ligand and interleukin-11 are clustered in humans. SCGF was shown to be expressed in bone and bone marrow (BM) by whole body *in situ* hybridization.[3] Although SCGF alone does not exhibit colony-stimulating activity, it does have a burst-promoting activity (BPA) and a granulocyte/macrophage (GM) colony-promoting activity (GPA) on erythroid and GM progenitor cells (BFU-E and CFU-GM) in a primary semisolid clonal culture in combination with erythropoietin (Epo) and GM colony-stimulating factor (GM-CSF), respectively, as well as a CFU-GM-supporting activity during short-term liquid culture of BM cells. However, the significance of SCGF in human hematopoiesis *in vivo* has not been fully elucidated.

Stem cell transplantation (SCT) provides an opportunity to trace the process of hematopoietic reconstitution *in vivo*, as stem cells given to a recipient following myeloablative therapy proliferate and differentiate until stable hematopoiesis is achieved.[4] Many cytokines are known to control this process of hematopoiesis positively or negatively *in vivo*.[5] Although there have been a great deal of descriptions about serum cytokine levels following SCT, none of them directly reflects post transplant hematopoiesis. Serum cytokine levels can be affected by the administration of exogenous cytokines such as granulocyte colony-stimulating factor (G-CSF) and also correlate with transplant-related toxicity and graft-versus-host disease (GVHD), which has been demonstrated with interleukin-6 (IL-6).[6,7] As for other cytokines, serum stem cell factor (SCF) levels, for example, have shown no correlation with post-transplant engraftment,[8] and thrombopoietin (TPO) has a negative correlation with platelet counts and is affected by platelet transfusions.[9,10]

To monitor serum SCGF in the various settings of hematopoiesis *in vivo*, we have established an enzyme-linked immunosorbent assay (ELISA) to quantify human SCGF. Serum concentrations of SCGF, as well as those of SCF, TPO and IL-6, were measured in patients undergoing SCT. We found that the serum SCGF level significantly

Correspondence: Dr K Ando, Department of Hematology, Oncology and Rheumatology, Tokai University School of Medicine, Bouseidai, Isehara, Kanagawa 259-1193, Japan
Received 5 December 2002; accepted 13 March 2003

increased after SCT with or without GVHD and reflected hematopoiesis following SCT, so that it can serve as an indicator of hematopoietic recovery following SCT. By using RT-PCR analysis of SCGF gene expression, the major sources of serum SCGF were supposed to be both $CD34^+$ and $CD34^-CD33^+$ BM mononuclear cells, but not $CD34^-CD33^-$ cells, BM stromal cells or peripheral blood cells. This finding provides clinical evidence for serum SCGF as an indicator of hematopoietic recovery after SCT.

Materials and methods

Generation of monoclonal antibodies against human SCGF

Monoclonal antibodies (MoAbs) against human SCGF were raised using the synthesized peptide, REWEGGWG GAQEEEREREAL (human SCGF (6–26)), and recombinant human SCGF as the immunogen. Five week-old female SD rats (SLC, Shizuoka, Japan) were immunized by i.p. injection of 100 μg of the peptide coupled to keyhole limpet hemocyanin (KLH; Carbiochem, San Diego, CA), with 2 mg of aluminum gel and 10^9 cells of *Bordetella pertussis* (Serum Institute, Chiba, Japan) as adjuvant, per animal. Six-week-old female Balb/c mice (CLEA Co., Tokyo, Japan) were immunized by i.p. injection of 50 μg of the recombinant human SCGF per animal with the same adjuvant used for the synthesized peptide. The animals were killed 3 or 4 days after the last injection. The spleen cells were fused with P3.X63/Ag8.U1 (P3.U1), at a 10:1 ratio of spleen cells to P3.U1 cells, in PEG 1000 by the method of Kohler and Milstein[11] with some modifications. The antibody activity in the cultured supernatants from each well of the hybridoma was tested by binding ELISA. Positive wells were subcloned twice by the limiting dilution method. We finally obtained two MoAbs, designated as KM2142 and KM2804. KM2142 was raised against the synthesized peptide, and the other was against the recombinant human SCGF. Both MoAbs, KM2142 and KM2804, reacted specifically with the recombinant human SCGF (Figure 1a,b).

Enzyme immunoassay for detection of SCGF

A sandwich EIA for plasma Ox-LDL was done with a 96-well microtiter plate as the solid phase, with KM2142 antibody as the capture antibody, with biotinylated KM2804 as the second antibody and avidin–alkaline phosphatase as the indicator enzyme. Figure 1c is a typical calibration curve generated by plotting the absorbance at 415 nm *vs* the logarithm of the concentration of each calibrator.

Performance of ELISA

Serum samples serially diluted gave results close to linearity, indicating that the assay was quantitative and confirming parallelism between the standard and plasma samples.

Serum samples containing low (18.2 ng/ml), medium (58.2 ng/ml) and high (130.5 ng/ml) SCGF were supplemented with potentially interfering agents at various concentrations. There was no substantial interference from lipid up to 5 g/l (in terms of TG), from hemoglobin up to 5 g/l, from direct and indirect bilirubin up to 200 mg/l.

The working range of the assay was established by calculating the coefficient of variation (CV) of each calibrator in five independent calibration curves. The CV obtained for each calibrator from 2.7 to 175.0 ng/ml was $<10\%$.

The assay variation in the present EIA was examined using serum samples that contained SCGF at three different levels (18.2 ng/ml, 58.2 and 130.5 ng/ml). The

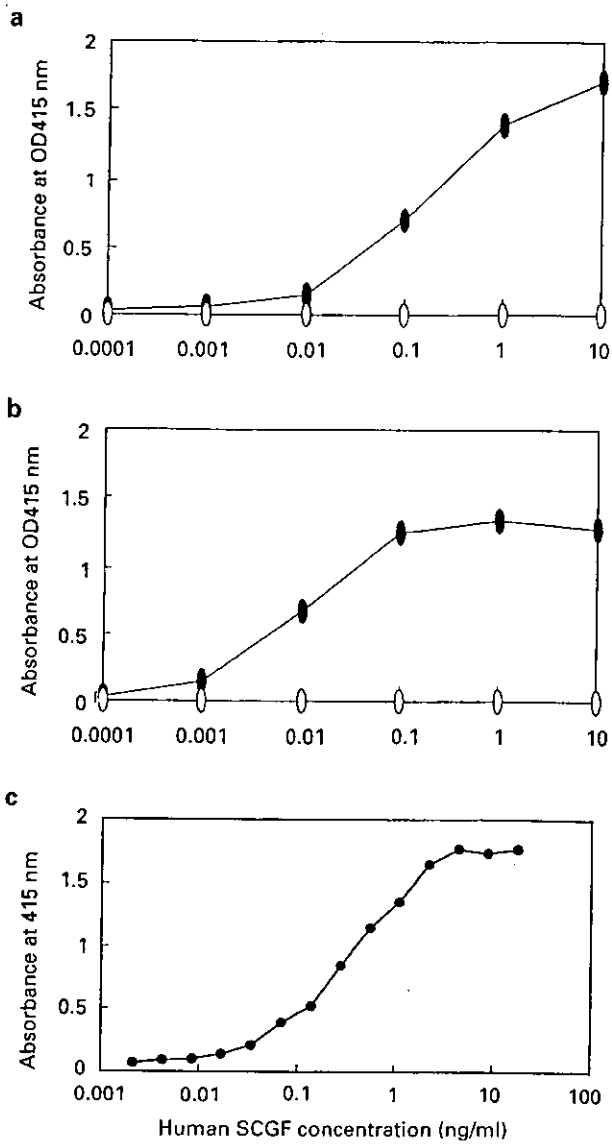

Figure 1 ELISA for human SCGF protein in serum. (**a,b**) Specificity of MoAbs in binding ELISA. Binding ELISA for KM2142(a) and KM2804(b) was performed using recombinant human SCGF(•) or BSA(○). (c) Titration curve of human SCGF by sandwich ELISA. Various concentrations of human SCGF were measured by sandwich ELISA using KM2142 and biotinylated KM2804. Each concentration of the calibrators was as follows: 140, 70, 35, 17.5, ...0.0042, 0.0021 ng/ml.

CVs within assay and between assay were 1.6–2.5% ($n=10$) and 2.2–6.3 % ($n=5$), respectively. To determine the analytical recovery, SCGF (19.8 and 98.0 ng/ml) was mixed with the serum samples containing 19.4 and 72.8 ng/ml SCGF (1:9). Recoveries of SCGF ranged from 95.7 to 109.7% (19.4 ng/ml) and from 98.2 to 100.8% (72.8 ng/ml), respectively.

Patients

The subjects were 27 patients who underwent SCT from January 1997 to July 2001 in our institution. In all, 21 patients received allogeneic SCT, while the remaining six received autologous SCT, 14 of the patients who received allogeneic SCT developed acute GVHD. Patient characteristics, type of transplant, conditioning regimen, recovery of BM and GVHD are given in detail in Table 1. The status of the disease at SCT was complete remission in all patients. No relapse was observed during the study period. The median time from BMT to absolute neutrophil count (ANC) >500, platelet count >50000 and duration of using G-CSF were 11, 14.5 and 13 days for autologous SCT patients. Those of the patients with and without GVHD were 16, 24.5, 22 and 14, 21 and 15, respectively. Acute GVHD was clinically diagnosed using the criteria described by Glucksberg *et al.*[12]

Measurement of cytokines

All cytokines were measured by ELISA at four time points as Takatsuka *et al.*[13] previously described. (1) before SCT; (2) during the aplastic phase after SCT (day 1–7); (3) during the rapid granulocyte recovery phase (days 8–21 in allogeneic SCT patients and days 9–17 in autologous patients); and (4) at the time of granulocyte stabilization after discontinuation of G-CSF (days 20–40 in allogeneic SCT patients and days 15–27 in autologous patients).

Serum SCF, TPO and IL-6 levels were measured in duplicate using ELISA kits (human SCF and TPO ELISA kits; R&D Systems, Minneapolis, MN, USA and human IL-6 ELISA kit; BioSource International, Camarillo, CA, USA). Minimum detectable levels of SCF, TPO and IL-6 were 31.2, 31.2 and 15.6 pg/ml, respectively.

Statistical analysis

All results are expressed as mean value plus or minus s.d.'s. The paired or unpaired Student's *t*-test was used to

Table 1 Clinical features of the patients

Patient no.	*Age/ Sex*	*Diagnosis*	*Type of transplant*	*Conditioning regimen*	*Duration of G-CSF used*	*Days from BMT to ANC>500*	*Days from BMT to Plt>50000*	*Acute GVHD (organ)*
Allogeneic transplantation								
1	24/F	NHL	sPBSCT	TBI/VP-16/CY	5–19	9	15	–
2	16/M	CML	uBMT	TBI/VP-16/CY	5–26	15	25	–
3	52/F	SAA	sBMT	TAI/CY	5–17	16	23	–
4	44/F	ALL	sPBSCT	TBI/Ara-C/CY	5–17	15	17	–
5	17/M	AML	uBMT	TBI/CY	5–26	14	21	–
6	33/M	MDS	sPBSCT	TBI/CY	5–18	13	>100	–
7	22/F	CML	sPBSCT	TBI/VP-16/CY	5–21	13	13	–
8	32/M	ALL	sPBSCT	TBI/VP-16/CY	5–17	11	17	Grade3 (skin, gut, liver)
9	23/M	ALL	uBMT	TBI/VP-16/CY	5–12	18	22	Grade2 (gut)
10	42/F	ALL	sBMT	TBI/VP-16/CY	5–27	22	37	Grade1 (skin)
11	26/M	ALL	sPBSCT	TBI/VP-16/CY	5–21	12	16	Grade1 (skin)
12	38/F	CML	sBMT	TBI/VP-16/CY	5–29	18	28	Grade1 (skin)
13	44/F	AML	uBMT	TBI/VP-16/CY	5–26	15	26	Grade1 (skin)
14	28/M	ALL	uBMT	TBI/VP-16/CY	5–21	15	25	Grade2 (skin, gut)
15	46/M	CML	sPBSCT	TBI/VP-16/CY	5–27	15	23	Grade3 (skin, gut)
16	35/F	MDS	uBMT	TBI/VP-16/CY	5–26	19	>100	Grade1 (skin)
17	23/M	ALL	uBMT	TBI/VP-16/CY	5–22	15	17	Grade1 (skin)
18	37/M	AML	sBMT	TBI/AraC /CY	5–21	21	50	Grade3 (skin, gut)
19	37/M	AML	sPBSCT	TBI/AraC	5–22	17	>100	Grade1 (skin)
20	20/M	MDS	uBMT	TBI/CY	5–26	15	38	Grade3 (skin, gut)
21	35/M	AML	uBMT	TBI/CY	5–32	16	36	Grade1 (skin)
Autologoua sterm cell transplanation								
22	44/M	NHL	PBSCT	MCNU/CBDCA/VP-16/CY	(–)	9	9	
23	34/M	NHL	PBSCT	MCNU/CBDCA/CY	5–7	9	14	
24	39/M	NHL	PBSCT	L-pam/CY/VP-16/Dex	5–20	11	14	
25	33/M	NHL	PBSCT	L-pam/CY/VP-16/Dex	5–9	10	15	
26	62/M	NHL	PBSCT	L-pam/CY/VP-16/Dex	5–20	11	32	
27	55/F	NHL	PBSCT	L-pam/CY/VP-16/Dex	5–17	12	18	

G-CSF = granulocyte colony stimulating factor; BMT = bone marrow transplantation; ANC = absolute neutrophil count; Plt = platelets; GVHD = graft-versus-host disease; NHL = non-Hodgkin's lymphoma; CML = chronic myelocytic leukemia; SAA = severe aplastic anemia; ALL = acute lymohicytic leukemia; AML = acute myelocytic leukemia; MDS = myelodysplastic syndrome; sPBSCT = peripheral blood stem cell transplantation from sibling; uBMT = unrelated BM transplantation; sBMT = BM transplantation from sibling; TBI = total body irradiation; V P-16 = etoposide; CY = cyclophosphamide; TAI = thoracoabdominal irradiation; Ara-C = cytarabine; MCNU = ranimustine; CBDCA = carboplatin; L-pam = melphalan; Dex = dexamethasone.

determine the probability of significant differences when comparing two groups. P-values <0.05 were considered significant. The Pearson's correlation coefficient was utilized for correlation statistics.

Cells and cell culture

Peripheral blood and BM cells were obtained from four healthy volunteers, and mononuclear cells were separated from these samples. BM mononuclear cells were also separated into $CD34^+$ and $CD34^-$ cells using an immunomagnetic bead system (MACS, Miltenyi Biotec, Glodbach, Germany). $CD34^-$ cells were further fractionated into $CD34^-CD33^+$glycophorin A^-, $CD34^-CD33^-$glycophorin A^+, $CD34^-CD33^-$glycophorin A^- cells by sorting with a FACS Vantage™.

The CFU-C assay was performed as described previously[1]. All cultures were done in triplicate, and the number of CFU-C was scored at day 10 of culture. The colony types were determined by *in situ* observations using an inverted microscope.

A portion of BM mononuclear cells was cultured in RPMI 1640 medium supplemented with 10% heat-inactivated fetal bovine serum (FBS) at 37°C in a humid atmosphere with 5% CO_2. Half of the medium was recovered from 3 to 4 days, and adherent cells were collected as stromal cells.

RT-PCR

Total RNA was extracted from each type of cell using RNeasy Mini Kit (QIAGEN, Hilden, Germany). cDNA was synthesized from total RNA (1 μg) using the Super-Script First-Strand Synthesis System for RT-PCR (GIBCO BRL, Gaithesburg, MD, USA) and subjected to PCR. A fragment of SCGF cDNA (209bp) was amplified with the following primers: forward 5′-GTCCTCTTTTCCCTCAA CA-3′; and reverse 5′-TTTTGGGGGCTTTGGTGG-3′. The PCR conditions were as follows: denaturation at 94°C for 5 min, followed by 25 cycles consisting of denaturation at 94°C for 1 min, annealing at 61°C for 1 min, elongation at 72°C for 1 min, and final reaction at 72°C for 7 min. A fragment of G3PDH cDNA (546 bp) was amplified with the primers, 5′-CCCATCACCATCTTCCAGGAGC-3′ and 5′-TTCACCACCTTCTTGATGTCATCATA-3′. The PCR conditions were as follows: denaturation at 94°C for 5 min, followed by 22 cycles consisting of denaturation at 94°C for 1 min, annealing at 55°C for 1 min, and elongation at 72°C for 1 min, and final reaction at 72°C for 7 min. The PCR products were analyzed on 2% agarose gels, stained with SYBR Green I Nucleic Acid Gel Stains (TaKaRa, Kyoto, Japan), and viewed under UV light.

Results

SCGF levels in normal volunteers and patients before SCT

The serum SCGF level in normal volunteers was 13.0 ± 2.6 ng/ml. ($n=10$), while those in patients before autologous SCT and allogeneic SCT were 19.27 ± 6.11 and 9.75 ± 6.8 ng/ml respectively. The serum SCGF level in autologous SCT patients was significantly higher than those in normal volunteers and allogeneic SCT patients ($P<0.02$). In autologous SCT patients, four of six patients received G-CSF within 1 month of sampling time.

SCGF levels after SCT

The serum SCGF levels gradually increased after SCT (Figure 2). The maximum level of serum SCGF was observed during rapid granulocyte recovery and then the level decreased to the pre transplant level in autologous SCT patients (Figure 2a). SCGF levels before and after autologous SCT were 19.28 ± 6.11 ng/ml and 36.55 ± 15.67 ng/ml ($n=6$) ($P<0.01$) (Table 2). The serum SCGF levels in allogeneic SCT patients increased until the time of granulocyte stabilization (Figure 2b). SCGF levels before and after allogeneic SCT were 9.76 ± 6.81 and 25.01 ± 15.14 ng/ml ($n=21$) ($P<0.001$). In patients with and those without GVHD after allogeneic SCT (Figure 2c, d), there was no difference in SCGF levels after SCT (23.23 ± 10.78 ng/ml ($n=14$) *vs* 26.84 ± 19.86 ng/ml ($n=7$)). Hence, the presence of GVHD did not affect the serum level of SCGF. The source of hematopoietic stem cells did not affect the serum level of SCGF after SCT either (24.65 ± 12.87 ng/ml in BMT ($n=13$) (Figure 2e) *vs* 25.69 ± 19.84 ng/ml in PBSCT ($n=8$) (Figure 2f)).

It is noteworthy that in two patients (nos. 18 and 19) serum SCGF did not increase in either phase after SCT. In these patients, engraftment was delayed.

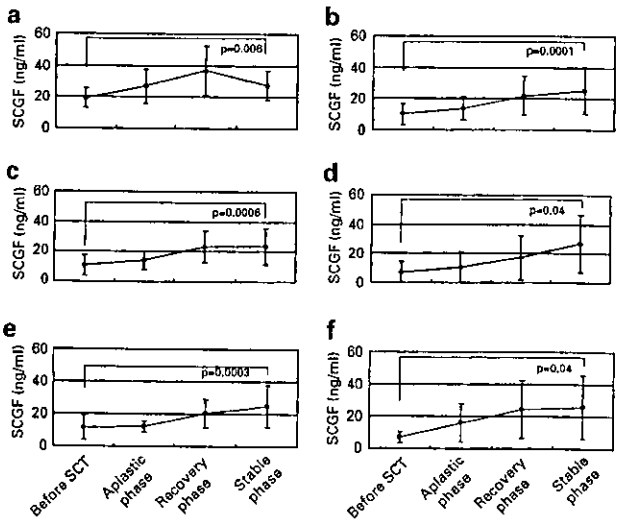

Figure 2 Serum SCGF levels before and after various types of SCT. Serum SCGF was measured by ELISA on four occasions as Takatsuka *et al.*[13] previously described: (1) before SCT; (2) during the aplastic phase after SCT (days 1–7); (3) during the rapid granulocyte recovery phase (days 8–21 in allogeneic SCT patients and days 9–17 in autologous patients); and (4) at the time of granulocyte stabilization after discontinuation of G-CSF (days 20–40 in allogeneic SCT patients and days 15–27 in autologous patients). (a) autologous SCT patients; (b) all allogeneic SCT patients; (c) allogeneic SCT patients with GVHD; (d) allogeneic SCT patients without GVHD; (e) allogeneic BMT patients; (f) allogeneic PBSCT patients.

Table 2 Cytokine levels of serum during SCT

	Before SCT	*After SCT*	*P-value*
SCGF (ng/ml)			
Auto	19.275±6.113	36.554±15.669	<0.01
Allo	9.757±6.807	25.011±15.135	<0.001
GVHD (+)	10.8±6.741	23.23±10.783	<0.001
GVHD (−)	7.325±6.912	26.842±19.861	<0.05
BMT	11.432±7.615	24.648±12.867	<0.001
PBSCT	6.646±3.66	25.685±19.835	<0.05
SCF (pg/ml)			
Auto	656.608±168.049	796.009±199.629	
Allo	829.400±247.139	808.990±264.220	
TPO (pg/ml)			
Auto	446.37±179.475	1603.356±533.877	<0.001
Allo	715.504±478.449	1771.146±1116.981	<0.02
IL-6 (pg/ml)			
Auto	2.693±1.933	15.395±11.678	<0.04
GVHD (+)	12.116±15.29	175.982±113.654	<0.02
GVHD (−)	10.225±13.842	97.316±86.676	<0.04

SCT = stem cells transplantation; SCGF = stem cell growth factor; Auto = autologous transplantation; Allo = allogeneic transplantation; GVHD = graft-versus-host disease; BMT = bone marrow transplantation; PBSCT = peripheral blood stem cell transplantation; SCF = stem cell factor; TPO = thrombopoietin.

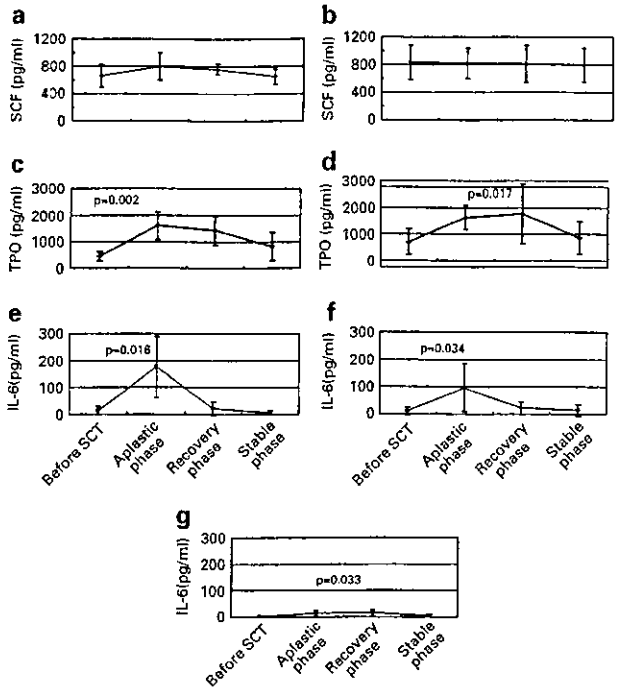

Figure 3 Serum SCF, TPO and IL-6 levels before and after SCT. Serum SCF, TPO and IL-6 were measured by ELISA on four occasions: (1) before SCT; (2) during the aplastic phase after SCT (days 1–7); (3) during the rapid granulocyte recovery phase (days 8–21 in allogeneic SCT patients and days 9–17 in autologous patients); and (4) at the time of granulocyte stabilization after discontinuation of G-CSF (days 20–40 in allogeneic SCT patients and days 15–27 in autologous patients). (a) SCF levels in autologous SCT patients; (b) SCF levels in allogeneic SCT patients; (c) TPO levels in autologous SCT patients; (d) TPO levels in allogeneic SCT patients; (e) IL-6 levels in allogeneic SCT patients with GVHD; (f) IL-6 levels in allogeneic SCT patients without GVHD; (g) IL-6 levels in autologous SCT patients.

SCF levels during SCT

The serum SCF levels did not change significantly during the observation period in autologous or in allogeneic SCT patients (Figure 3a, b). SCF levels after autologous SCT and allogeneic SCT were 796.0±199.62 pg/ml ($n=7$) and 808.99±264.22 pg/ml ($n=16$), respectively, and there was no significant difference among the two groups ($P>0.2$) (Table 2). Therefore, GVHD did not affect the serum level of SCF.

TPO levels during SCT

Serum TPO levels rapidly increased to the maximum value after autologous SCT, and then decreased to the pretransplant level in the stable phase (Figure 3c, d). In autologous transplant patients, the serum TPO gradually increased and reached the maximum value in the aplastic phase. TPO levels before and after autologous SCT were 446.37±179.48 pg/ml and 1603.36±533.88 pg/ml ($n=6$) ($P<0.001$) (Table 2). In allogeneic SCT patients, the maximum level of TPO was observed during rapid granulocyte recovery. TPO levels before and after allogeneic SCT were 715.5±478.45 pg/ml and 1771.15±1116.98 pg/ml ($n=7$) ($P<0.02$) (Table 2).

IL-6 levels during SCT

In allogeneic SCT patients with and those without GVHD, serum IL-6 levels rapidly increased to the maximum value in aplastic phase and returned to the basal level before the recovery phase (Figure 3e, f) ($n=7$, 6). Therefore, the maximum level of IL-6 was observed before acute GVHD and there was no significant difference between the two groups ($P=0.18$). Since many allogeneic SCT patients had high fever and their serum CRP concentrations increased during the aplastic phase, it seems that the high serum IL-6 levels were also related to infection ($r=0.69$). In autologous SCT patients, serum IL-6 levels before SCT were 2.69±1.93 pg/ml, whereas they increased to 15.40±11.68 pg/ml during the rapidly granulocyte recovery and decreased to 5.09±4.57 pg/ml at the time of granulocyte stabilization (Figure 3g) ($n=6$). Serum IL-6 levels increased very slightly although four autologous SCT patients had fever and increase of serum CRP concentrations during the aplastic phase. Serum IL-6 levels in autologous SCT patients were significantly lower than those in allogeneic SCT patients ($P<0.05$). Therefore, not only infection but also the GVH reaction affected the serum level of IL-6.

The source of human SCGF production

In order to elucidate the types of BM cells expressing SCGF, we carried out RT-PCR analysis and a clonogenic assay using peripheral blood cells and BM cells from 4

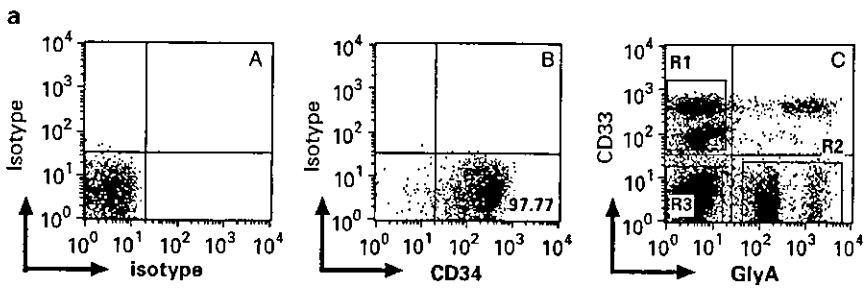

c

	CD34$^+$ (/400 cells)	CD34$^-$CD33$^+$GlyA$^-$ (/5000 cells)	CD34$^-$CD33$^-$GlyA$^+$ (/5000 cells)	CD34$^-$CD33$^-$GlyA$^-$ (/5000 cells)
CFU-Mix	43.5 ± 12.7	0	0	0
CFU-GM	39.3 ± 4.8	59.7 ± 6.6	0	0
BFU-E	58.3 ± 4.8	0	0	0
CFU-G	5.8 ± 1.0	10.3 ± 2.1	0	0
CFU-M	3.8 ± 1.0	3 ± 1	0	0
CFU-C	150.5 ± 18.8	73 ± 6.6	0	0

Figure 4 RT-PCR analysis of human SCGF in various types of cells. (a) CD34$^+$ cells were isolated by immunomagnetic column as 98% pure fraction (B). CD34$^-$ BM mononuclear cells were sorted into three subpopulations; CD34$^-$CD33$^+$glycophorin A$^-$ (R1), CD34$^-$CD33$^-$glycophorin A$^+$ (R2), CD34$^-$CD33$^-$glycophorin A$^-$ (R3) cells (C). The purity of sorted cells was more than 98%. Isotype control was shown (A). (b) RT-PCR analysis of each cell fraction. Negative control: RT-PCR without RT. Positive control (P.C.): Mo7e cell lines. PB: peripheral blood. BM: total BM mononuclear cells. 34+: CD34$^+$ BM cells, 33+: CD34$^-$CD33$^+$glycophorinA$^-$BM cells, GPA: CD34$^-$CD33$^-$glycophorin A$^+$ BM cells, TN:CD34$^-$CD33$^-$glycophorin A$^-$ BM cells. BM stromal cells 1–5 indicated cells from five different normal volunteers. (c) Clonogenic cell assay. All cultures were done in triplicate and the number of CFU-C was scored at day 10 of culture. The colony types were determined by *in situ* observations using an inverted microscope.

healthy volunteers in four independent experiments. SCGF was expressed in total BM mononuclear cells, BM CD34$^+$ and CD34$^-$CD33$^+$ cells, but not in CD34$^-$CD33$^-$ glycophorin A$^+$, CD34$^-$CD33$^-$glycophorin A$^-$ cells, BM stromal cells and peripheral blood mononuclear cells (Figure 4). The clonogenic ability of these fractions of BM cells was examined and found only in CD34$^+$ and CD34$^-$CD33$^+$ cells ($n=4$). CD34$^+$ cells produced CFU-GEMM, CFU-GM and BFU-E, while CD34$^-$CD33$^+$ cells produced only CFU-GM, CFU-GM and CFU-M. The plating efficiency was 37.5% in CD34$^+$ cells and 1.5% in CD34$^-$CD33$^+$ cells. Therefore, the cell populations expressing SCGF in BM mononuclear cells possess the colony-forming cell abilities.

Discussion

We established a sandwich ELISA to quantify SCGF, a new growth factor of primitive hematopoietic progenitor cells. The serum level of SCGF in normal volunteers (13.0 ± 2.6 ng/ml) was quite high when compared with other hematopoietic cytokines such as SCF or TPO.[14,15]

Moreover, we actually measured serum cytokines levels in patients undergoing SCT using this assay. In most patients serum SCGF levels gradually increased after SCT. Regardless of the presence of GVHD or type of transplant, SCGF levels significantly increased after SCT. Serum SCGF levels did not correlate with serum CRP levels ($r=0.02$), nor with granulocyte ($r=0.34$) or platelet count ($r=-0.13$) in the peripheral blood. The maximum level of SCGF was observed during the rapid granulocyte recovery phase in autologous patients, and during the granulocyte stabilization phase in allogeneic SCT patients, so that serum SCGF levels began to rise earlier in autologous SCT patients than in allogeneic SCT patients. Among allogeneic patients, serum SCGF levels in PBSCT patients began to rise earlier than in BMT patients. The recovery of hematopoiesis following SCT is generally earlier in autologous patients than in allogeneic patients, and it is also earlier in PBSCT patients than in BMT patients. In this study, the median time from SCT to ANC > 500, Platelets > 50 000 and duration of G-CSF administration were 9,10.5 and 14.5 days in autologous SCT patients, and 18, 15, 23 days in allogeneic SCT patients. These data suggested that the kinetics of serum SCGF levels are associated with the recovery of hematopoiesis following SCT, although no single parameter correlated with serum SCGF. Two other findings mentioned below support this notion.

In autologous SCT patients, serum SCGF levels before SCT (mean 19.275 ng/ml) were significantly higher than in allogeneic SCT patients (mean 9.757 ng/ml) or normal controls ($P<0.01$). As four of six autologous SCT patients underwent PBSC harvest within a month before SCT, we thought that excess hematopoiesis was related to high serum SCGF levels.

Furthermore, in two patients (patients nos. 18 and 19) the serum SCGF levels did not increase during the observation period after SCT in this study and in these patients recovery of hematopoiesis was delayed, so that they depended on transfusion of platelets for more than 50 days. This suggests that in patients whose serum SCGF levels do not increase, hematopoiesis will take more time to recover following SCT.

In a previous mouse study[3] the expression of SCGF was shown to localize in BM, proliferating chondrocytes, the perichondrium and periosteum. Therefore, we further analyzed SCGF production in BM cells. The results of RT-PCR indicated that SCGF was expressed in whole BM mononuclear cells, BM $CD34^+$ and $CD34^-CD33^+$ cells, with clonogenic ability, but not in $CD34^-$glycophorin A^+, $CD34^-CD33^-$glycophorin A^- cells and peripheral blood mononuclear cells, which do not have a clonogenic ability. This implies that SCGF is produced by hematopoietic stem/progenitor cells and that serum SCGF may reflect the total number of stem/progenitor cells in BM. The precise role of SCGF in hematopoiesis *in vivo* requires further investigation.

TPO, SCF and IL-6 are other hematopoietic cytokines working during early hematopoesis.[16] Therefore, we measured the serum level of these cytokines together with SCGF in this study. Serum TPO levels markedly increased after SCT and gradually decreased as platelets recovered. Serum TPO levels were previously described to correlate inversely with platelet counts rather than with hematopoietic recovery. Serum SCF levels, in this study as well as other studies,[17] did not change after SCT. There was no specific association between serum SCF levels and hematopoiesis following SCT. IL-6 was described as an inflammatory cytokine and to correlate with serum level of CRP.[18] There was also a weak negative correlation of IL-6 with leukocyte or platelet counts. In this study, most patients showed elevation of serum IL-6 levels during the aplastic phase. Serum IL-6 levels in autologous SCT patients were significantly lower than those in allogeneic patients. Serum IL-6 levels indicate the presence of an inflammatory reactions, such as infection and GVHD, rather than hematopoiesis in these patients.

Although many cytokines have been reported to have a role in hematopoiesis, none of them directly reflects the status of post transplant hematopoiesis.[6–10,17,18] In this study, we demonstrate the parallel kinetics between serum SCGF levels and hematopoietic recovery after SCT. The time from SCT to the peak of serum SCGF levels differed according to the type of transplant, but after granulocyte stabilization those levels decreased in all cases. It is also suggested that in patients whose serum SCGF levels do not increase hematopoiesis will take much time to recover after SCT. The SCGF protein can be easily determined by ELISA, and the assay can be performed within several hours if a serum sample is available. Hence, SCGF can be a useful predictor of recovery of hematopoiesis following SCT.

Acknowledgements

We thank Drs Takashi Yahata, Hideyuki Matsuzawa and Yoshihiko Nakamura for technical assistance, members of Department of Hematology/Oncology of Tokai University for management of clinical samples.

References

1 Hiraoka A, Sugimura A, Seki T *et al.* Cloning, expression, and characterization of a cDNA encoding a novel human growth factor for primitive hematopoietic progenitor cells. *Proc Natl Acad Sci USA* 1997; **94**: 7577–7582.
2 Hiraoka A, Ohkubo T, Fukuda M. Production of human hematopoietic survival and growth factor by a myeloid leukemia cell line (KPB-M15) and placenta as detected by a monoclonal antibody. *Cancer Res* 1987; **47**: 5025–5030.
3 Hiraoka A, Yano K, Kagami N *et al.* Stem cell growth factor: *in situ* hybridization analysis on the gene expression, molecular characterization and *in vitro* proliferative activity of a recombinant preparation on primitive hematopoietic progenitor cells. *Hematol J* 2001; **2**: 307–315.
4 Weinthal JA. The role of cytokines following bone marrow transplantation: indications and controversies. *Bone Marrow Transplant* 1996; **18** (Suppl. 3): S10–S14.
5 Ogawa M. Differentiation and proliferation of hematopoietic stem cells. *Blood* 1993; **81**: 2844–2853.
6 Rowbottom AW, Riches PG, Downie C, Hobbs JR. Monitoring cytokine production in peripheral blood during acute graft-versus-host disease following allogeneic bone marrow transplantation. *Bone Marrow Transplant* 1993; **12**: 635–641.
7 Imamura M, Hashino S, Kobayashi H *et al.* Serum cytokine levels in bone marrow transplantation: synergistic interaction of interleukin-6, interferon-gamma, and tumor necrosis factor-alpha in graft-versus-host disease. *Bone Marrow Transplant* 1994; **13**: 745–751.
8 Cairo MS, Gillan ER, Weinthal J *et al.* Decreased endogenous circulating steel factor (SLF) levels following allogeneic and autologous BMT: lack of an inverse correlation with post-BMT myeloid engraftment. *Bone Marrow Transplant* 1993; **11**: 155–161.
9 Weisdorf DJ, DeFor T, Nichol J *et al.* Thrombopoietic cytokines in relation to platelet recovery after bone marrow transplantation. *Bone Marrow Transplant* 2000; **25**: 711–715.
10 Hamaguchi M, Yamada H, Morishima Y *et al.* Serum thrombopoietin level after allogeneic bone marrow transplantation: possible correlations with platelet recovery, acute graft-versus-host disease and hepatic veno-occlusive disease. *Nagoya Bone Marrow Transplantation Group. Int J Hematol* 1996; **64**: 241–248.
11 Kohler G, Milstein C. Continuous cultures of fused cells secreting antibody of predefined specificity. *Nature* 1975; **256**: 495–497.
12 Glucksberg H, Storb R, Fefer A *et al.* Clinical manifestations of graft-versus-host disease in human recipients of marrow from HLA-matched sibling donors. *Transplantation* 1974; **18**: 295–304.
13 Takatsuka H, Takemoto Y, Yamada S *et al.* Complications after bone marrow transplantation are manifestations of

systemic inflammatory response syndrome. *Bone Marrow Transplant* 2000; **26**: 419–426.
14 Molineux G, McNiece LK. Stem cell factor. In: Angus WT (ed.). *The cytokine handbook*. Academic Press: California, 1998, pp 713–725.
15 David JK. Thrombopoietin. In: Joost JO, Marc F(eds.). *Cytokine reference*. Academic Press: California, 2001, pp 965–982.
16 Rusten LS, Lyman SD, Veuby OP *et al*. The FLT3 ligand is a direct and potent stimulator of the growth of primitive and committed human CD34+ bone marrow progenitor cells *in vitro*. *Blood* 1996; **87**: 1317–1325.
17 Steffen M, Pichlmeier U, von dem Busche C, Zander A. Serum levels of stem cell factor in patients during transplantation of bone marrow or peripheral blood stem cells. *J Hematother Stem Cell Res* 2000; **9**: 55–61.
18 Steffen M, Durken M, Pichlmeier U *et al*. Serum interleukin-6 levels during bone marrow transplantation: impact on transplant-related toxicity and engraftment. *Bone Marrow Transplant* 1996; **18**: 301–307.